U.S. DEPARTMENT OF ENERGY
OFFICE OF CIVILIAN RADIOACTIVE WASTE MANAGEMENT

PRESENTATION TO THE NUCLEAR WASTE TECHNICAL REVIEW BOARD

SUBJECT: ROLE OF NONEQUILIBRIUM FRACTURE-MATRIX FLOW IN SITE CHARACTERIZATION

PRESENTER: DR. THOMAS A. BUSCHECK

PRESENTER'S TITLE AND ORGANIZATION: HYDROLOGIST
LAWRENCE LIVERMORE NATIONAL LABORATORY
LIVERMORE, CALIFORNIA

PRESENTER'S TELEPHONE NUMBER: (415) 423-9390

REGISTRY HOTEL, DENVER, COLORADO
JUNE 25-27, 1991

The role of nonequilibrium fracture-matrix flow in site characterization

- Motivation and scope of this presentation
- Fracture-matrix interaction: mathematical approximations
- Fracture-dominated versus matrix-dominated flow
- Fracture-dominated flow: the major flow regimes
- Fracture-dominated flow: episodic behavior
- Examples of fracture-matrix flow in Yucca Mountain
- Summary of fracture-matrix flow at Yucca Mountain
- Fracture-matrix flow: physical retardation of radionuclides
- The impact of repository-generated hydrothermal flow
- Conclusions

Motivation and Scope of this Presentation

Factors mitigating liquid flow along preferential fracture pathways

- Discontinuity in fracture networks
- Dispersion of liquid flow in fracture networks
- Fracture-matrix interaction

Fracture-matrix interaction: impact on flow

- Capillary imbibition from fracture to matrix
  - limits the vertical penetration of fracture flow
  - delays the impact of fracture flow
- Vapor-phase removal of moisture from matrix to fracture
  - facilitated by long matrix travel times

Fracture-matrix interaction: impact on transport

- Capillary imbibition from fracture to matrix
  - limits transport of radionuclides in fractures
  - mitigates vertical displacement of radionuclides (imbibed during earlier events) by subsequent episodic events
  - facilitates chemical retardation

Nonequilibrium fracture-matrix flow: supporting field evidence

- Norris (1989) measured "bomb pulse" ^{36}Cl at depths of 30-31, 52-54, and 152-153 *m* in USW UZ-1

- During heating and cooling of the G-Tunnel "Heater" test Ramirez and others (1989, 1990) did not observe any significant increase in saturation outside of the boiling zone

- Water potential and saturation measurements in USW UZ-7 indicate significant disequilibrium between welded and nonwelded units

Nonequilibrium fracture-matrix flow: fracture data

- Montazer and others (1985) determined bulk (air) permeability, k_b, in TSw (7×10^{-13} to $1 \times 10^{-11}\ m^2$)

- For well J-13 Thodarson (1983) reported a bulk hydraulic conductivity of 1 m/day ($k_b = 1.7 \times 10^{-11}\ m^2$)

  - For a matrix permeability of $1.9 \times 10^{-18}\ m^2$ obtained by Peters and others (1984), the cubic law yields the following fracture apertures for the assumed fracture spacings

Assumed fractures per meter	Fracture aperture μm
1.00	203 to 587
3.33	141 to 407
10.00	94 to 273
100.00	43 to 127

- The Environmental Assessment (1986) reports 15 to 40 fractures per cubic meter for TSw

For zero recharge flux the system is in gravity-capillary equilibrium, with the fractures drained of water above the water table

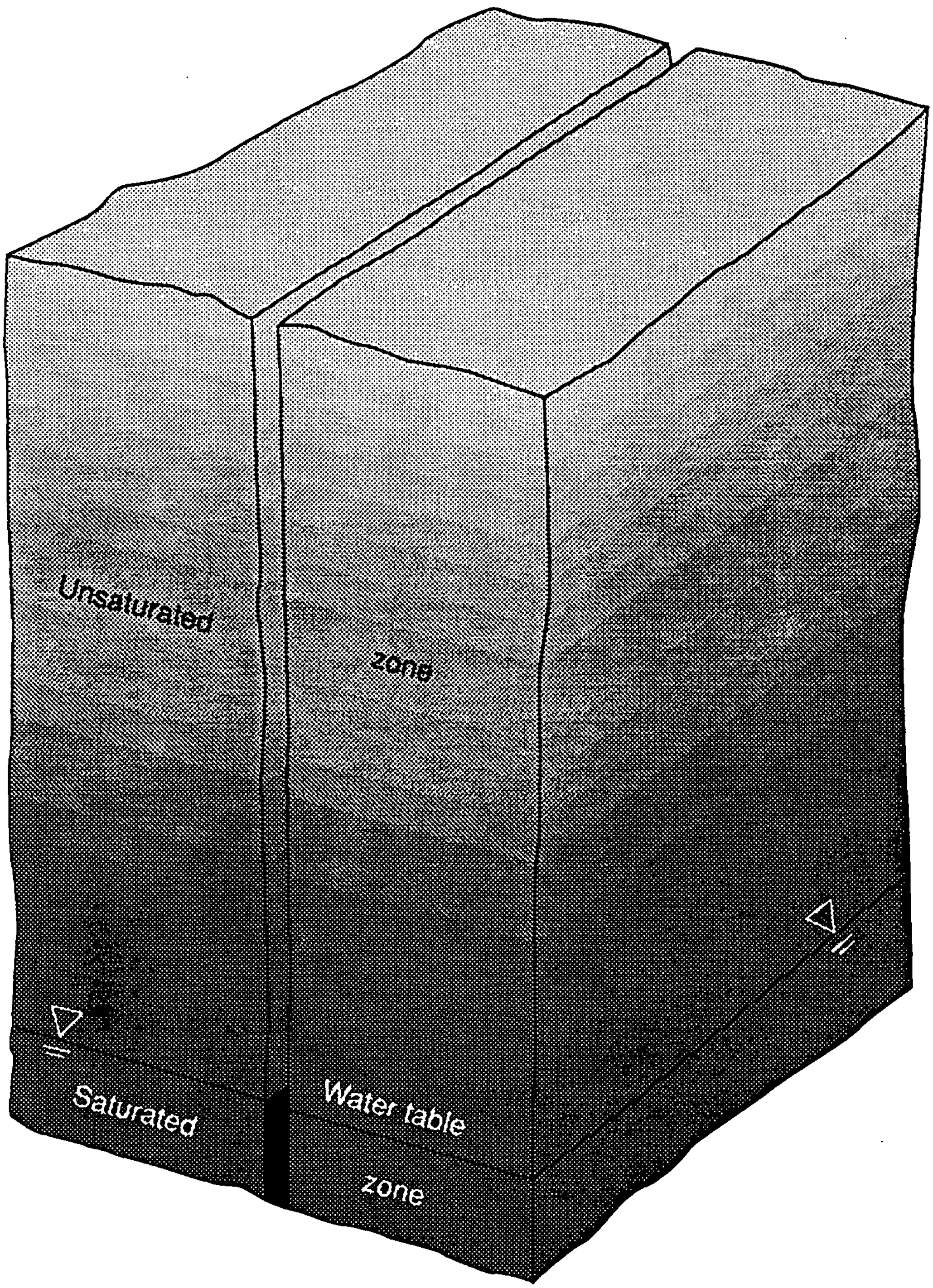

Vertical liquid saturation profile for various steady-state one-dimensional recharge fluxes versus saturations from the reference informance base

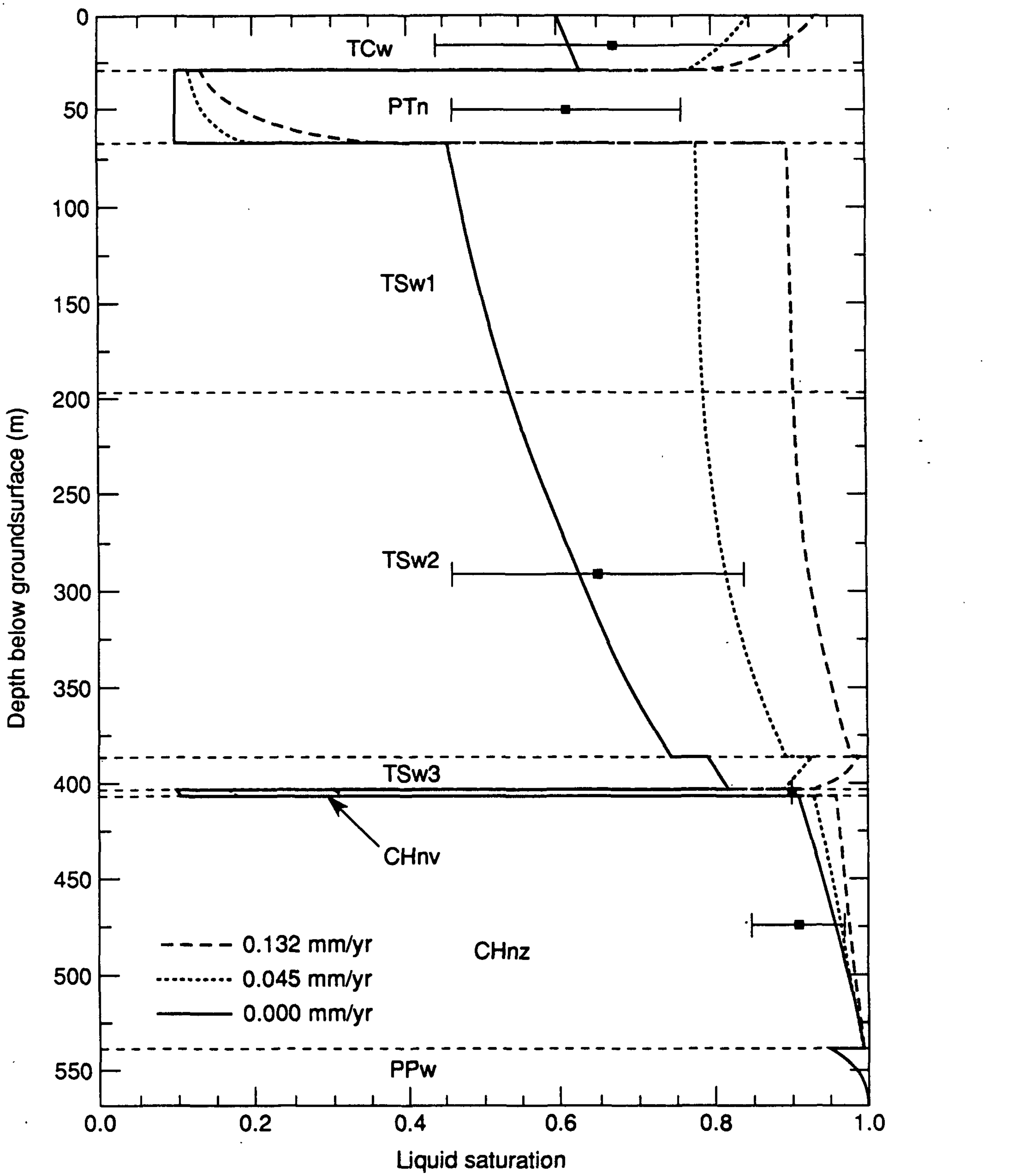

ES-TB-37 (6-10-91) IL

Vertical liquid saturation profile for zero recharge flux

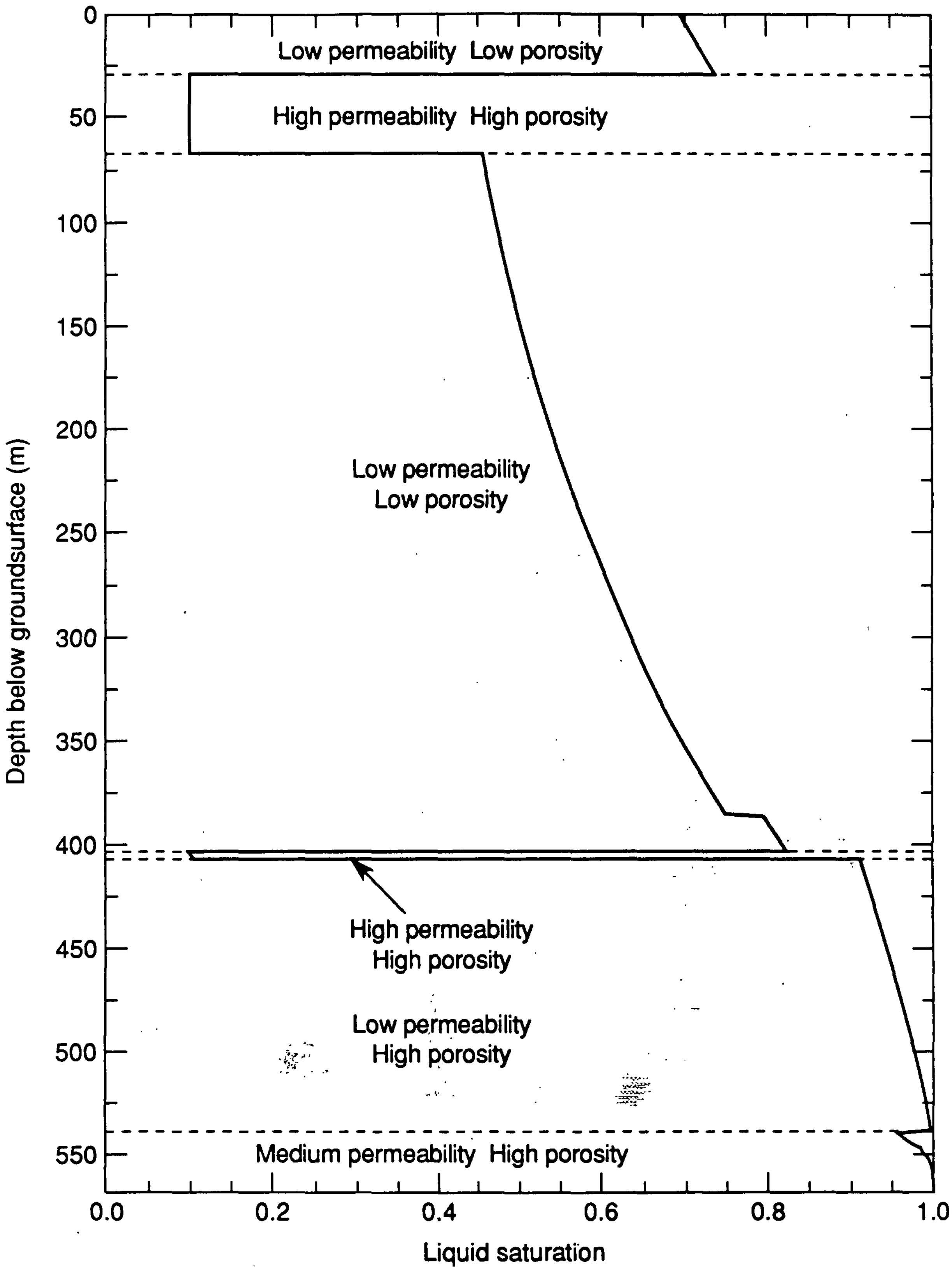

ES-TB-16 (2-17-91) IL

Liquid saturation distribution for zero recharge flux

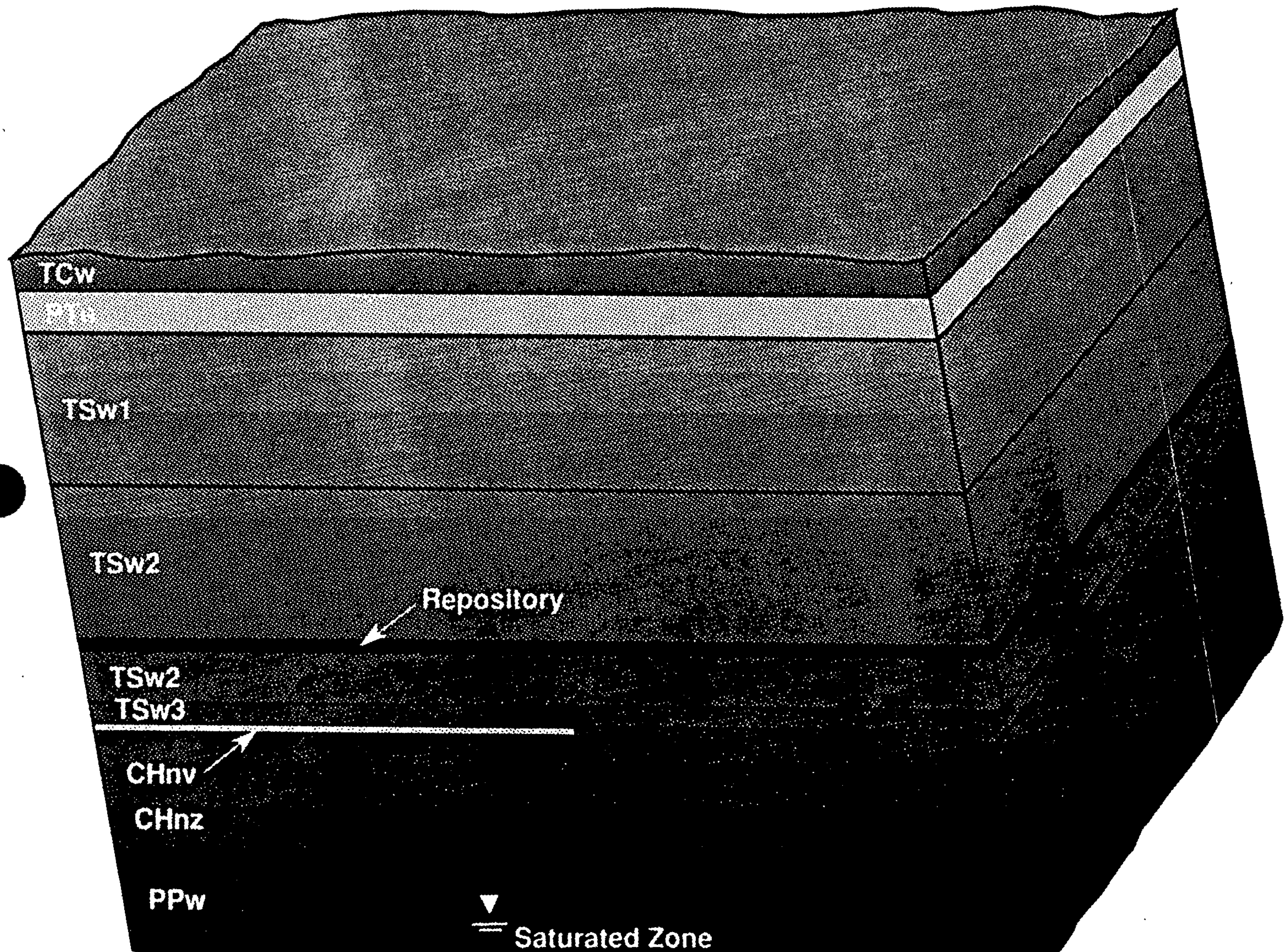

ES-TB-16x (3-4-91) FH

Liquid saturation distribution from reference information base indicates very positive recharge flux in nonwelded vitric PTn and CHnv

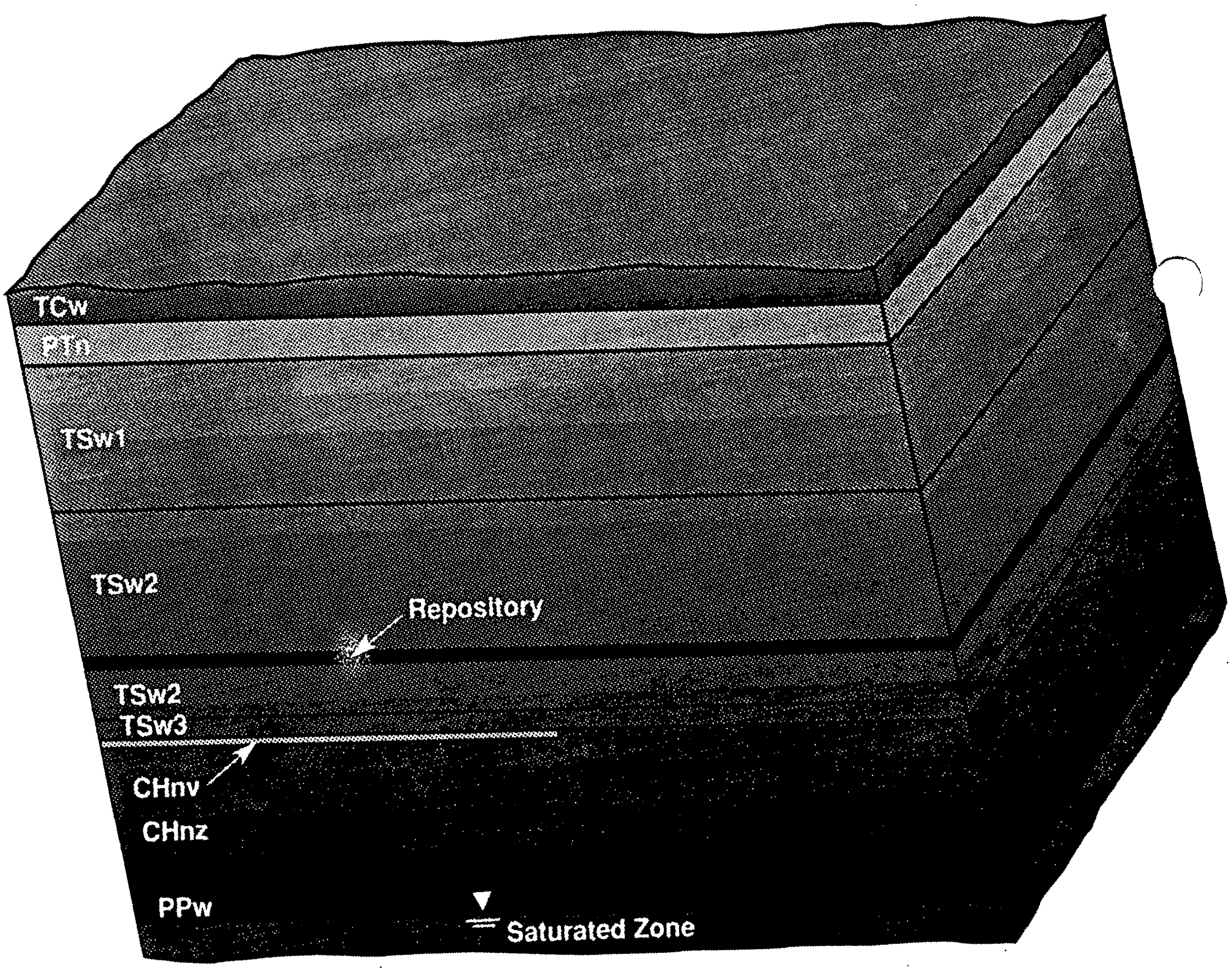

ES-TB-17 (3-4-91) FH

Fracture-Matrix Interaction: Mathematical Approximations

Fracture-matrix interaction has been treated by several approximations

Zeroth order approximation (Klavetter and Peters)

$$\psi_f = \psi_m$$

First order approximation (Warren and Root)

$$q_{fm} = C\,[\,\psi_f - \psi_m\,]$$

Second order approximation (Nitao and Buscheck)

$$\phi_f \frac{\partial S_f}{\partial t} = \frac{\partial}{\partial z} K_f k_r (S_f) \left[\frac{\partial \psi_f}{\partial z} - 1 \right] - q_{fm}$$

$$\phi_m \frac{\partial S_m}{\partial t} = \frac{\partial}{\partial z} \nabla \cdot K_m k_r (S_m) \left[\nabla \psi_m - \hat{z} \right] + q_{fm}$$

The equivalent continuum model assumes capillary equilibrium between fractures and matrix blocks, resulting in uniform porous media flow

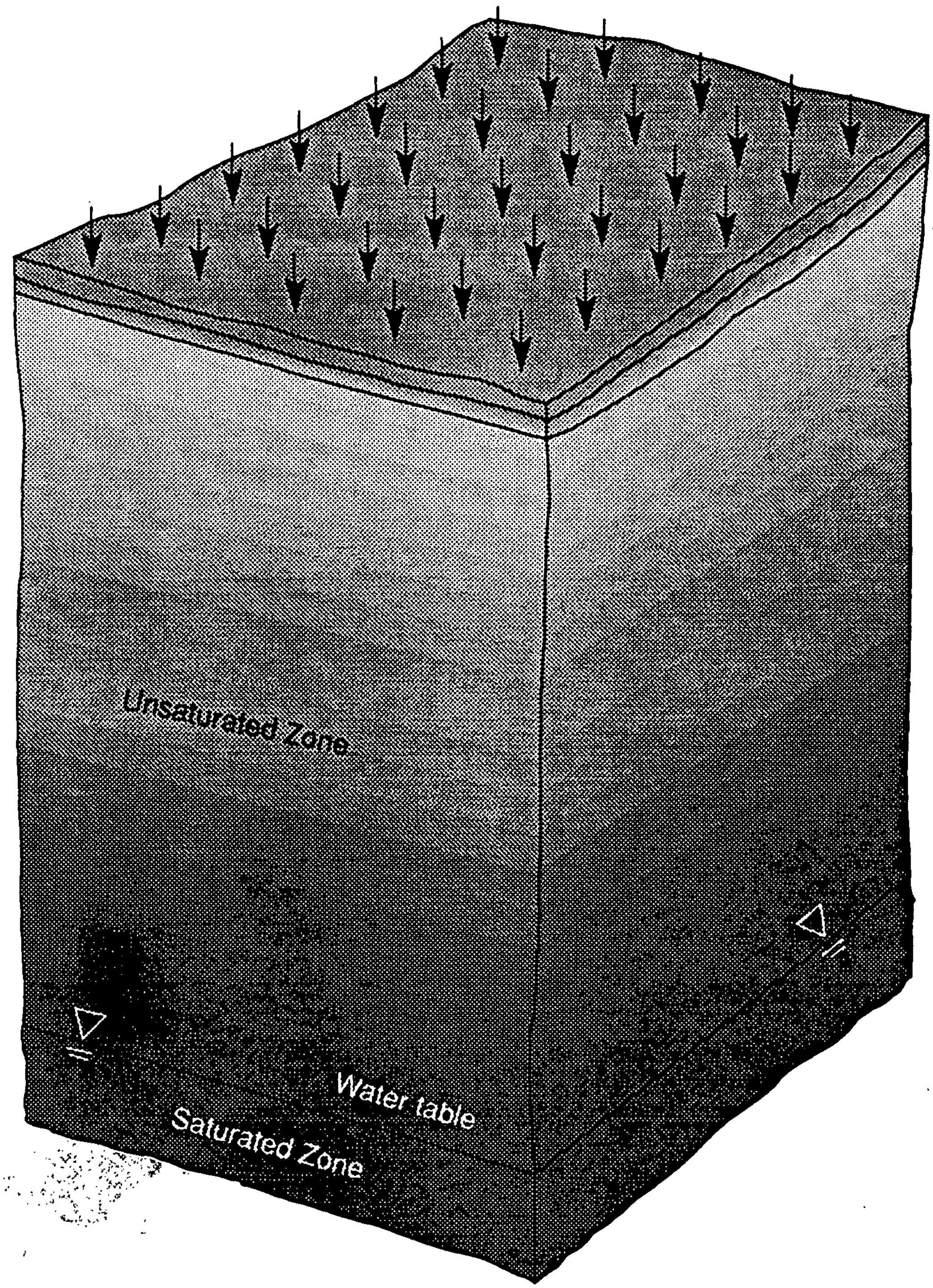

Episodic infiltration event causes capillary disequilibrium between fractures and matrix blocks

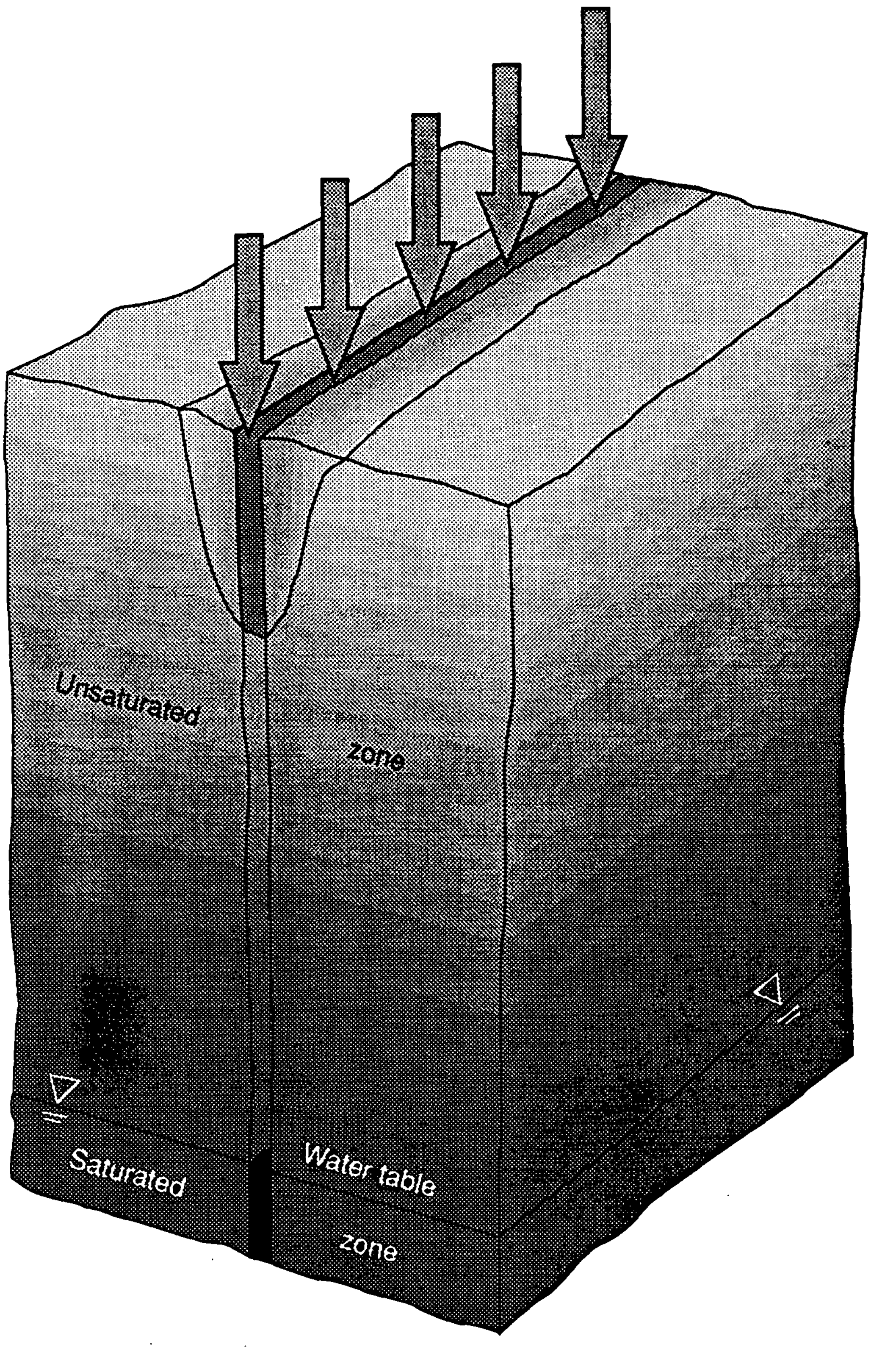

ES-TB-22 (2-18-91) FH

Fracture-Dominated Versus Matrix-Dominated Flow

Critical fracture aperture for matrix vs. fracture dominated flow

$b << b^*$

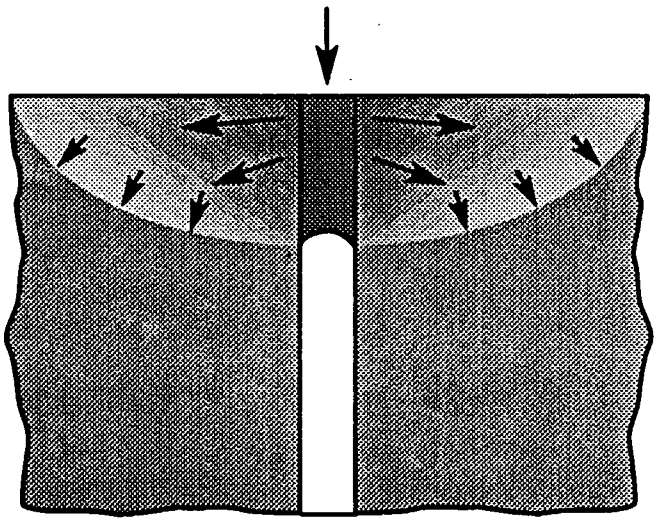

$b >> b^*$

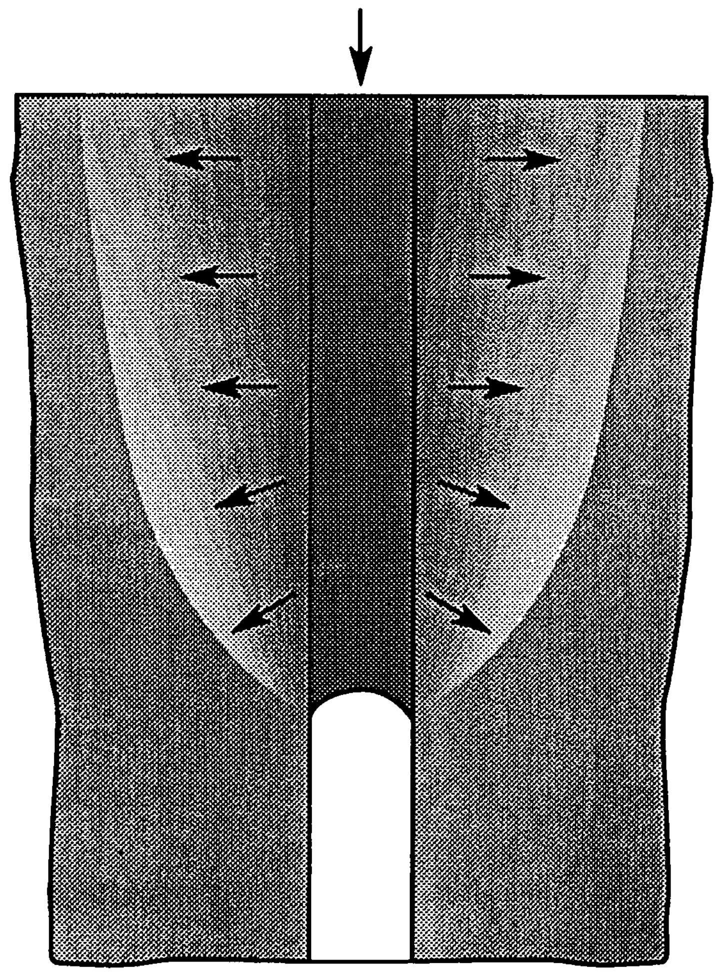

$$b^* = \left[\frac{12 \mu \phi (S - S_i) D_m}{\rho g} \right]^{1/3}$$

Topopah Spring Tuff

$b^* = 10\ \mu m$

Fracture-Dominated Flow: the Major Flow Regimes

ES-TB-14 (6-15-91) PM

Fracture-dominated flow consists of three flow regimes, corresponding to three flow periods

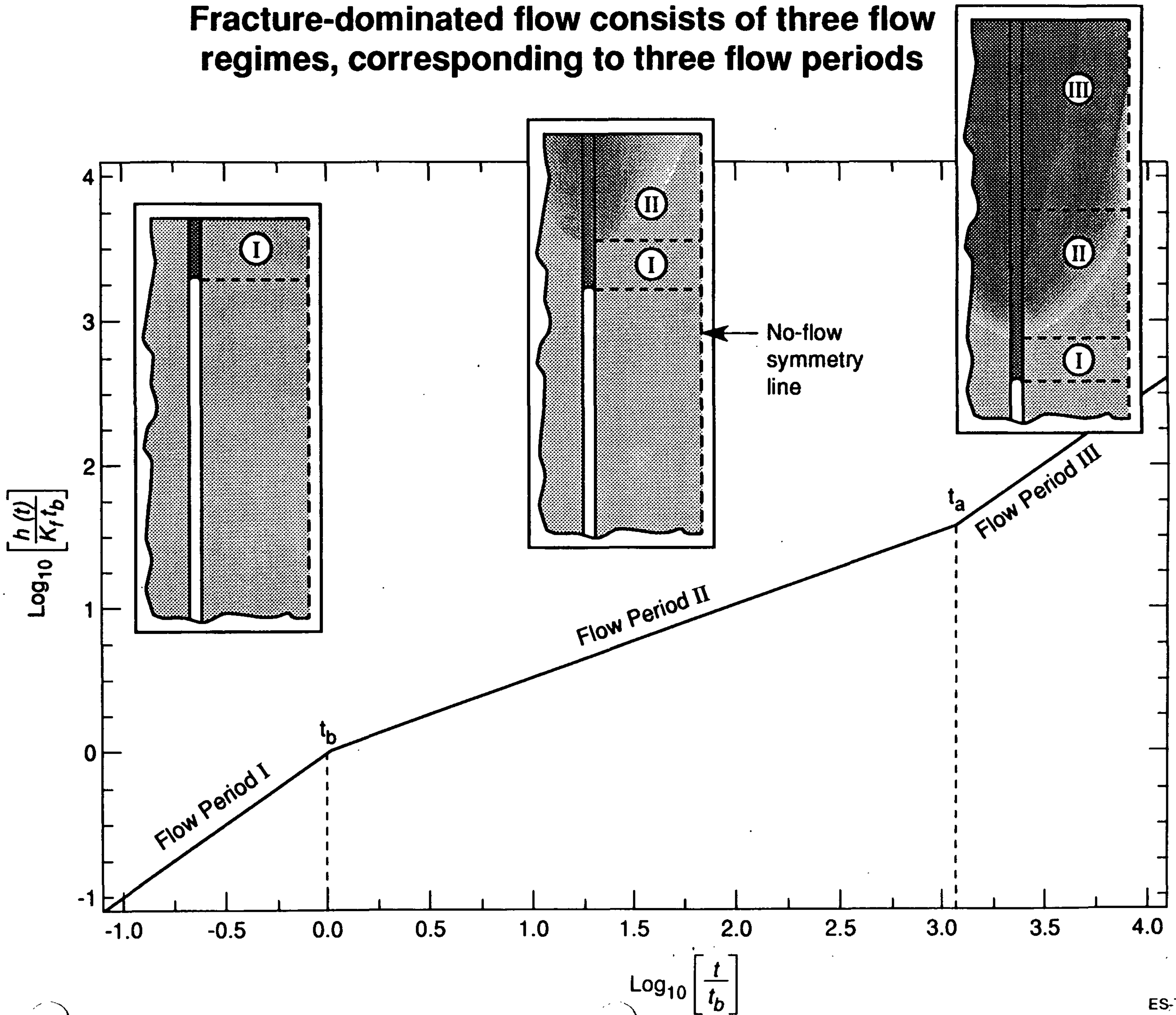

ES-TP-2 (3-2-91) IL

Fracture-matrix interaction retards the velocity of the liquid front, ranging from no retardation (Flow Period I) to maximal retardation (Flow Period III)

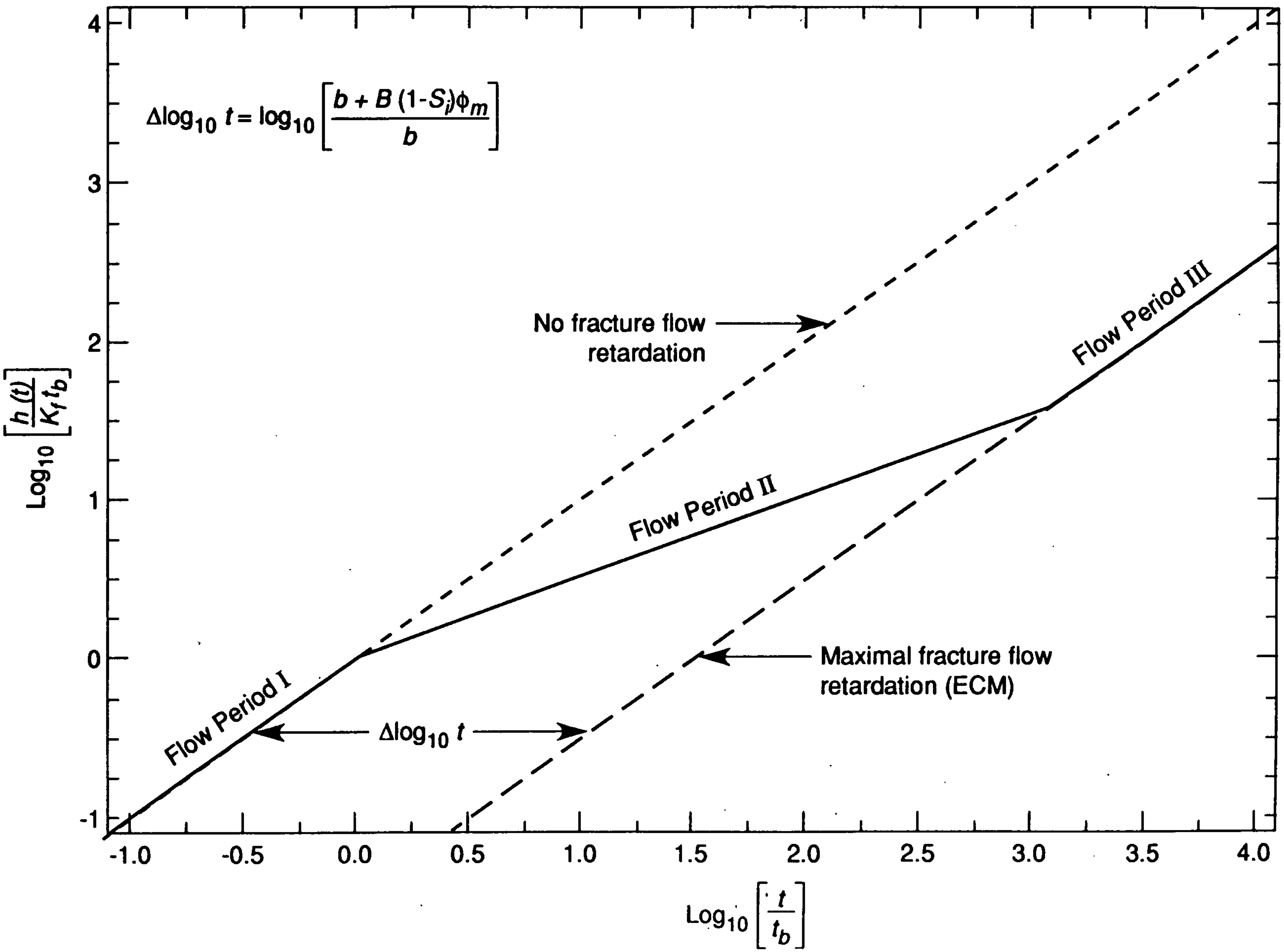

ES-TB-1 (3-2-91) IL

Fracture-Dominated Flow: Episodic Behavior

100 μm fracture; fracture spacing = 3.0 m
Dimensionless liquid saturation at t = 2 hours

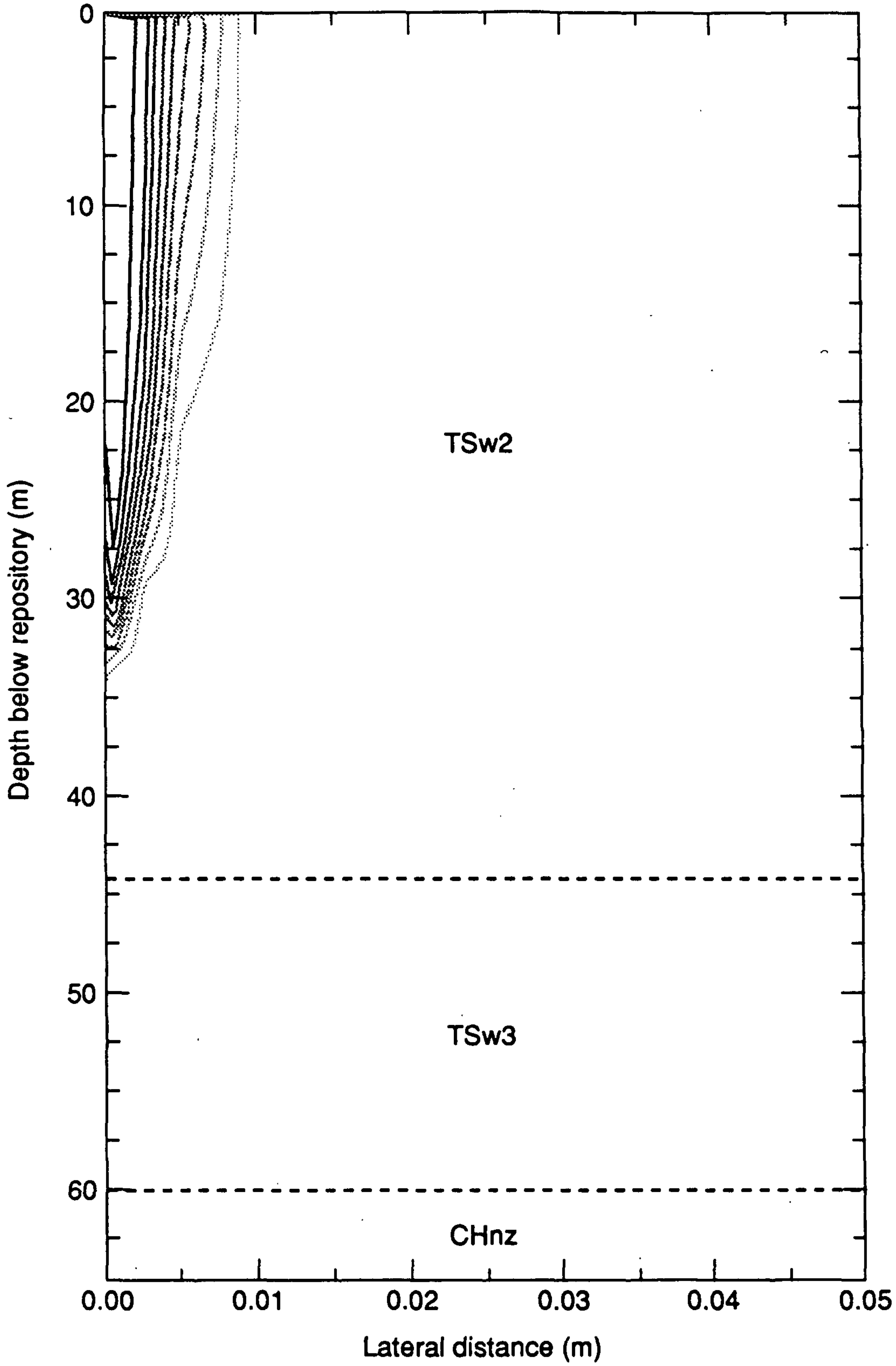

ES-TB-26 (2-19-91) IL

Equivalent continuum model of 100 μm fracture; fracture spacing = 3.0 m Dimensionless liquid saturation at t = 2 hours

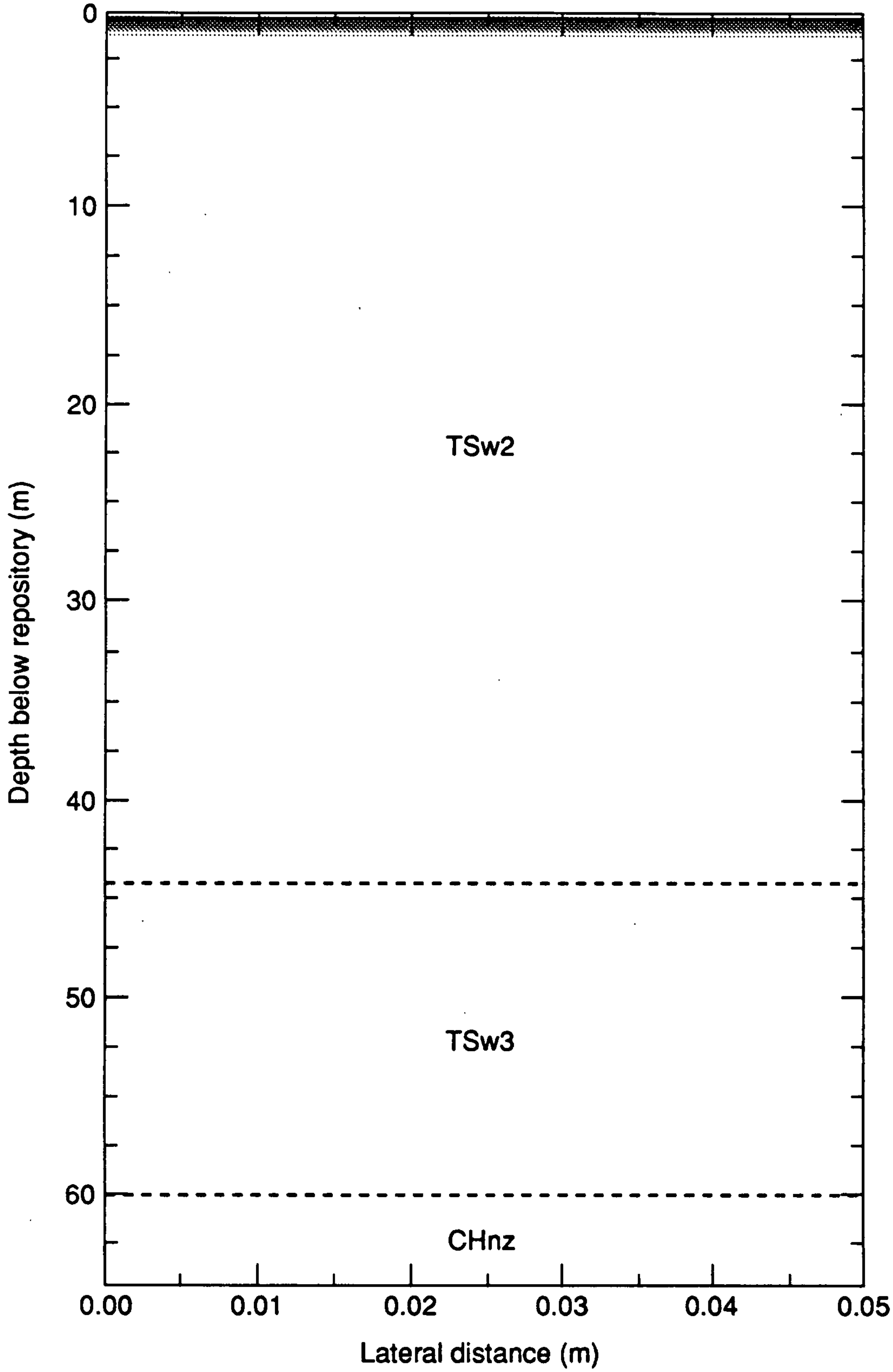

ES-TB-27 (2-19-91) IL

Liquid pulse in fracture is imbibed quickly by matrix following removal of infiltration source

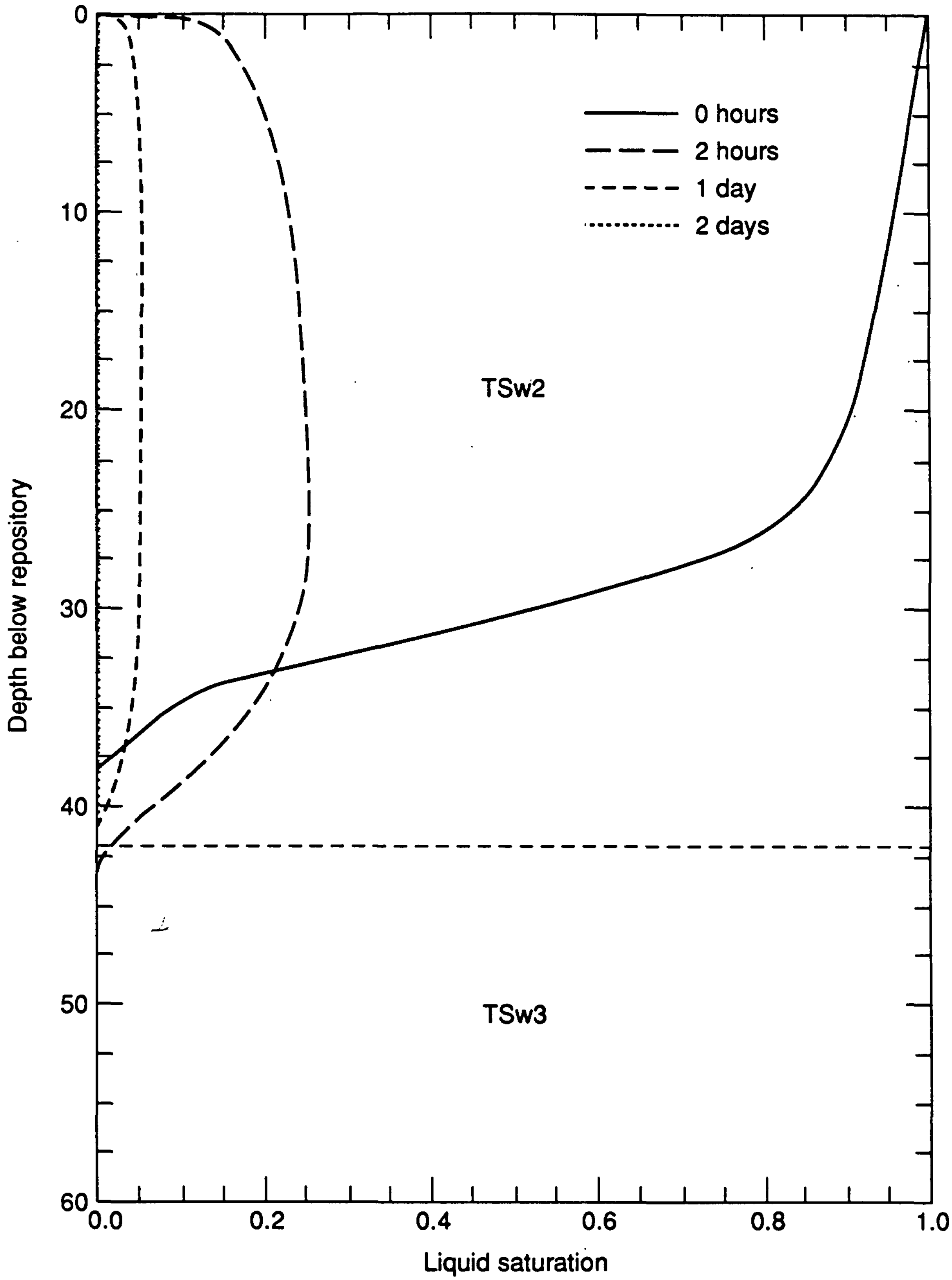

ES-TB-23 (2-19-91) IL

Liquid pulse in fracture is imbibed quickly by matrix following removal of infiltration source

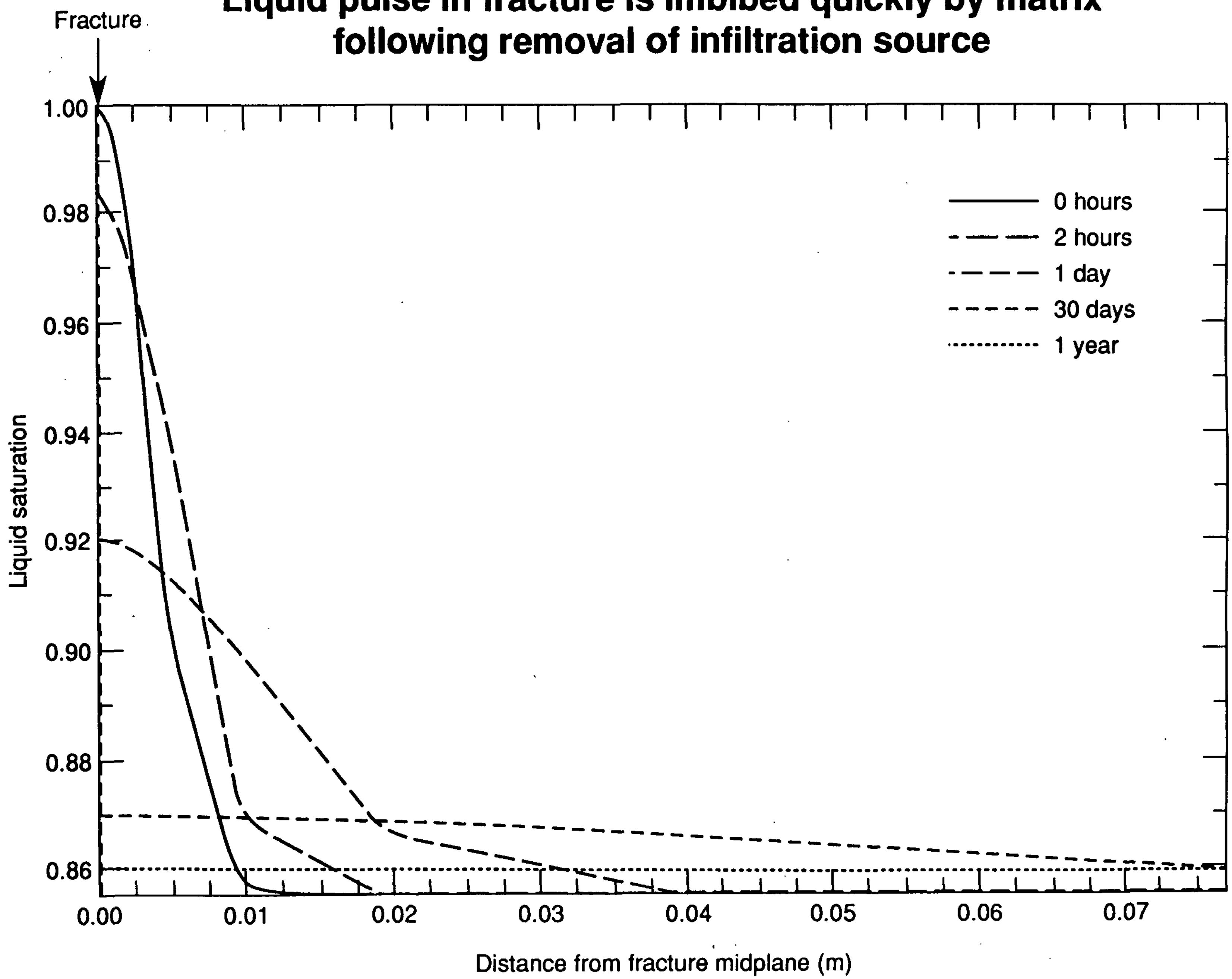

ES-TP-24 (2-18-91) IL

Examples of Fracture-Matrix Flow in Yucca Mountain

100 µm fracture; fracture spacing = 3.0 m
Dimensionless liquid saturation at t = 4 hours

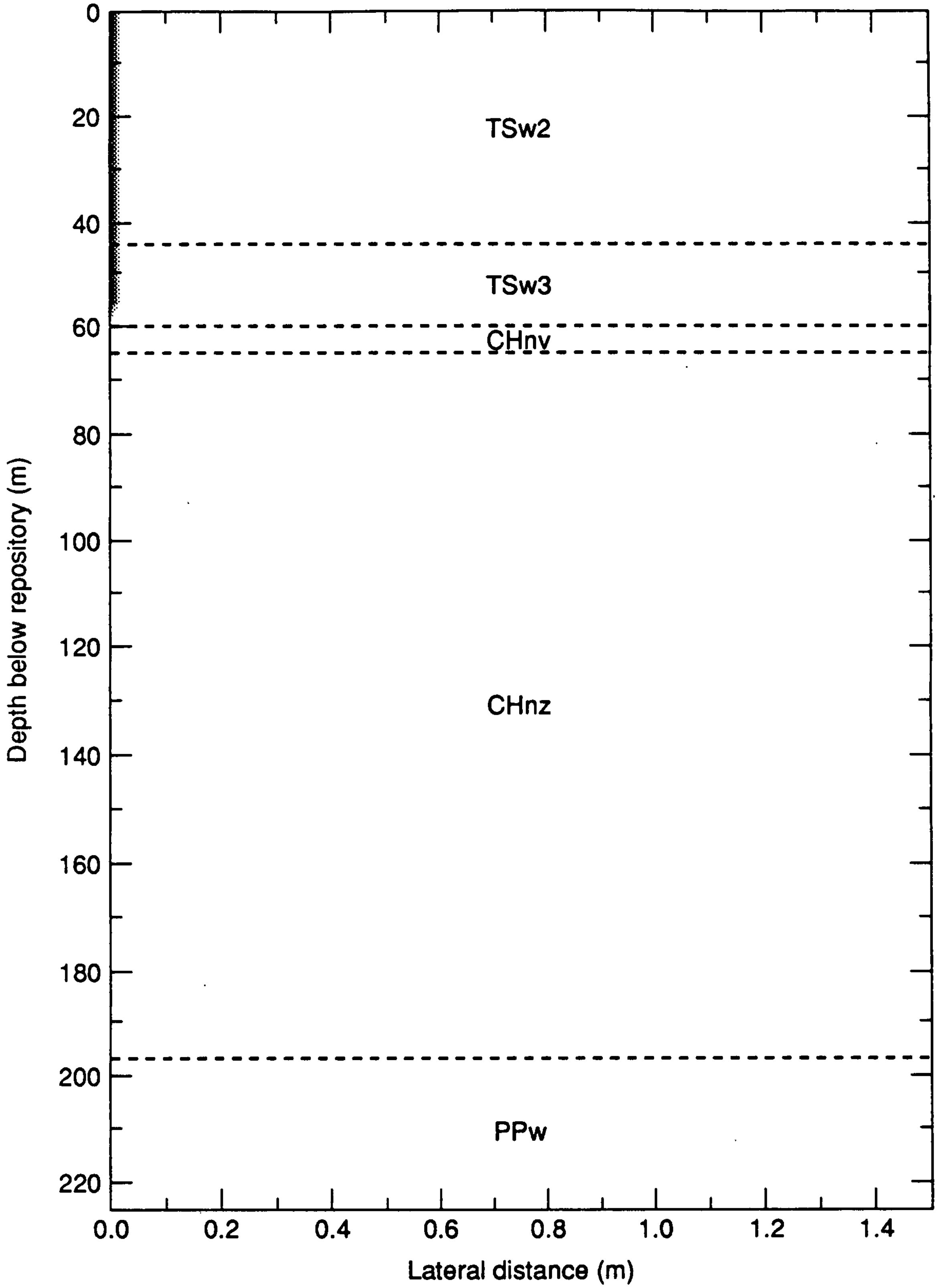

ES-TB-2 (2-16-91) IL

100 μm fracture; fracture spacing = 3.0 m
Dimensionless liquid saturation at t = 8 hours

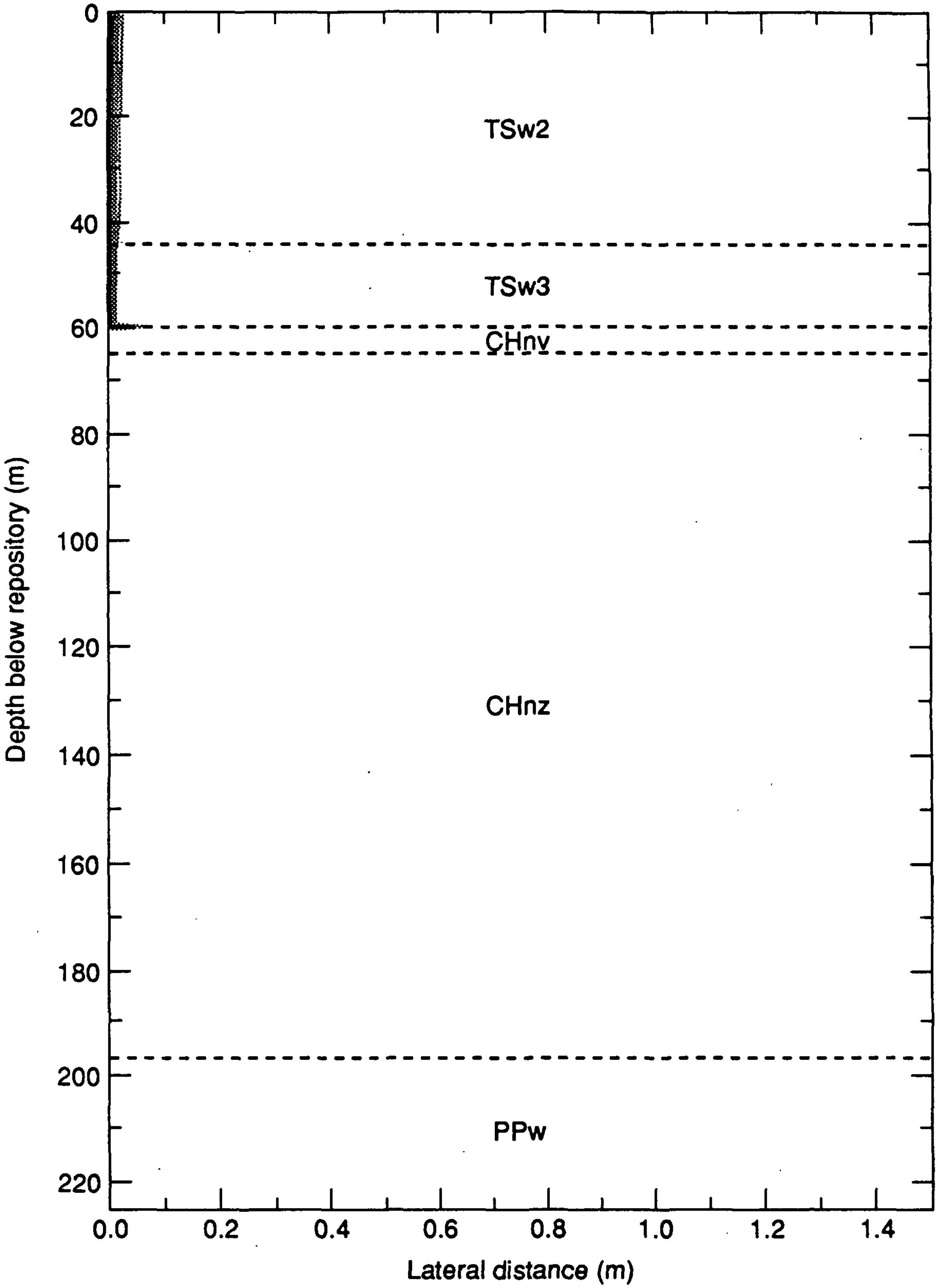

ES-TB-3 (2-16-91) IL

100 μm fracture; fracture spacing = 3.0 m
Dimensionless liquid saturation at t = 20 days

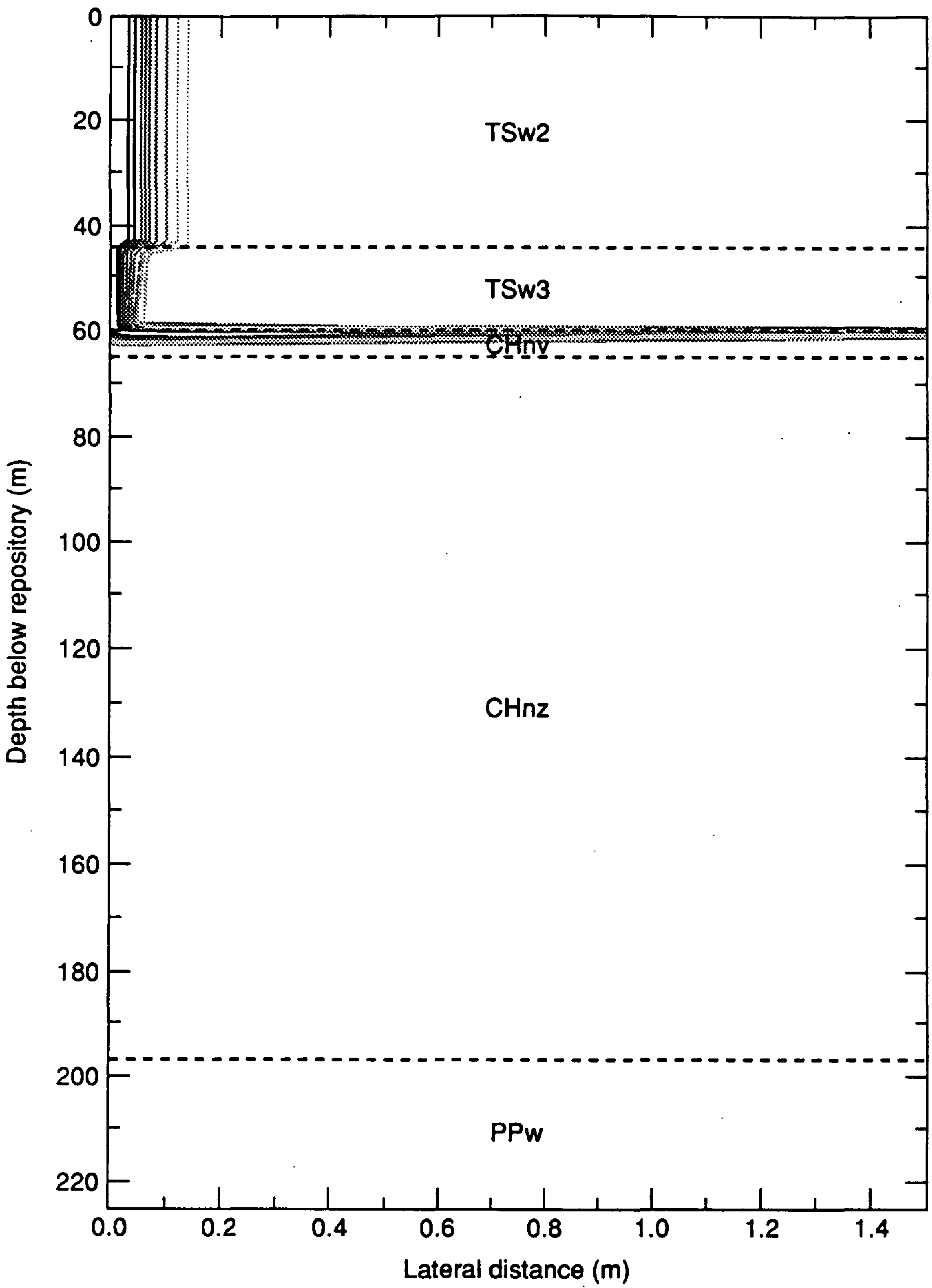

ES-TB-4 (2-16-91) IL

100 μm fracture; fracture spacing = 3.0 m
Dimensionless liquid saturation at t = 83 days

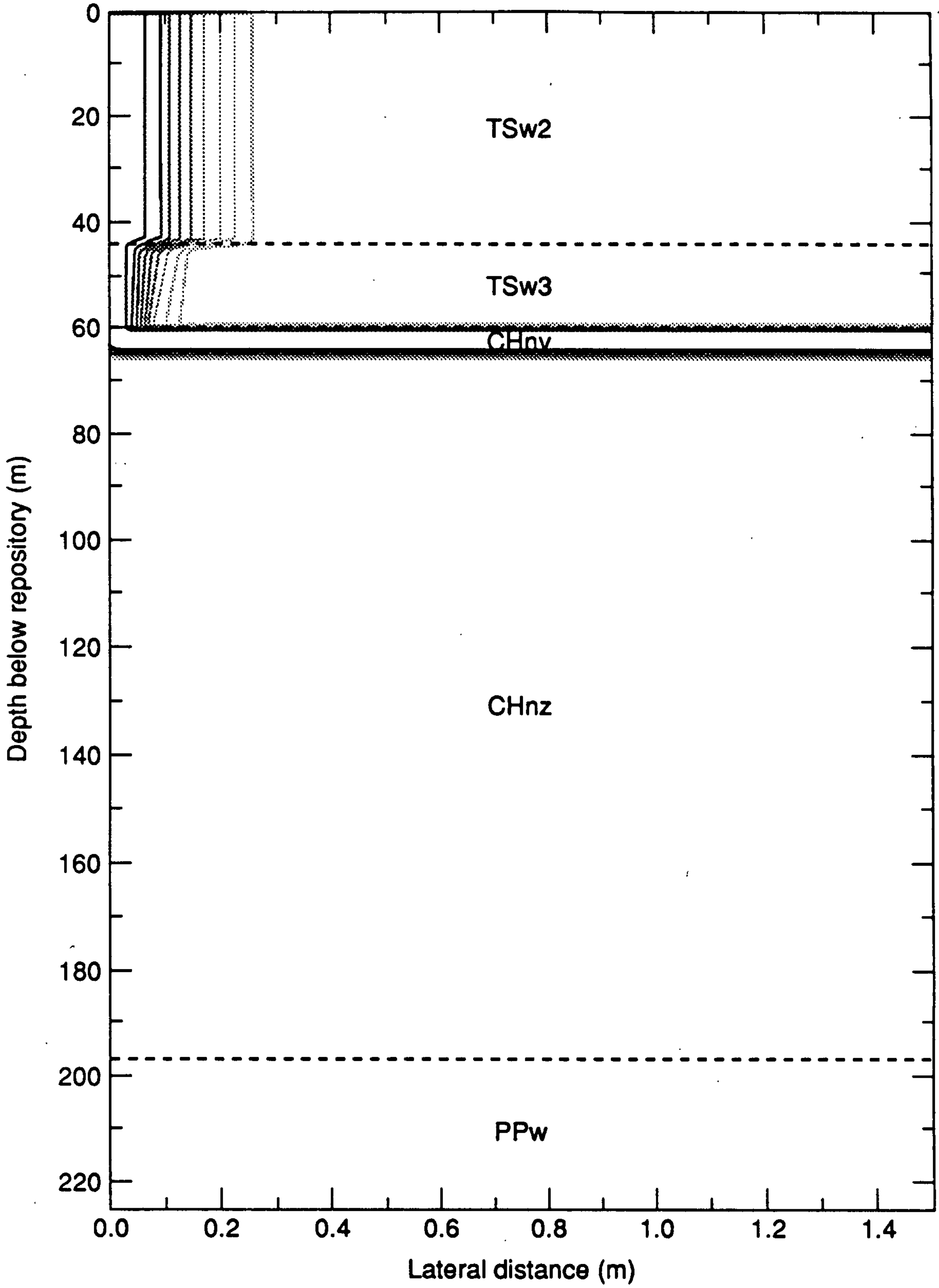

ES-TB-5 (2-16-91) IL

100 μm fracture; fracture spacing = 3.0 m
Dimensionless liquid saturation at t = 84 days

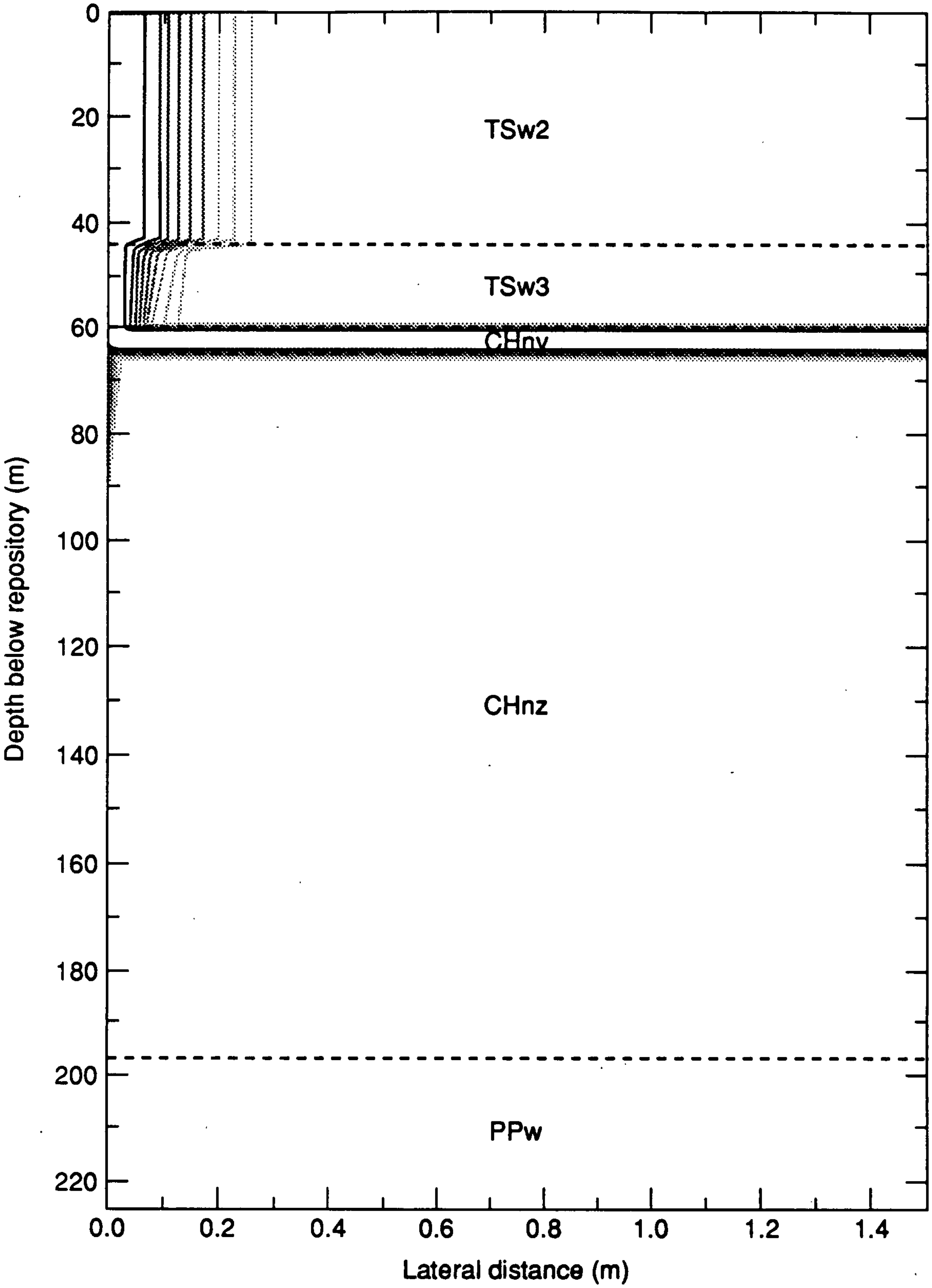

ES-TB-6 (2-16-91) IL

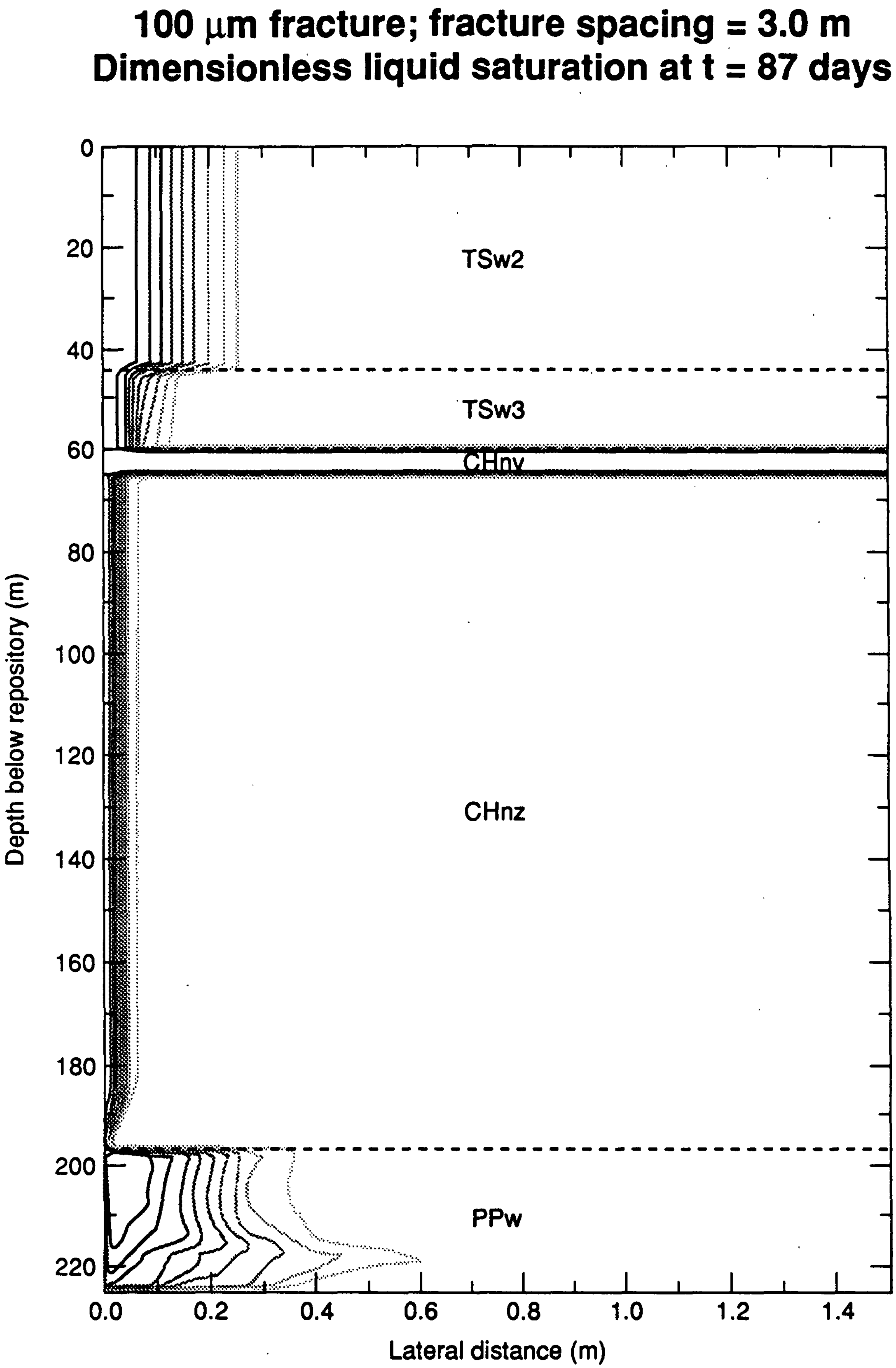

ES-TB-1 (2-16-91) IL

100 μm fracture; fracture spacing = 30 m
Dimensionless liquid saturation at t = 240 days

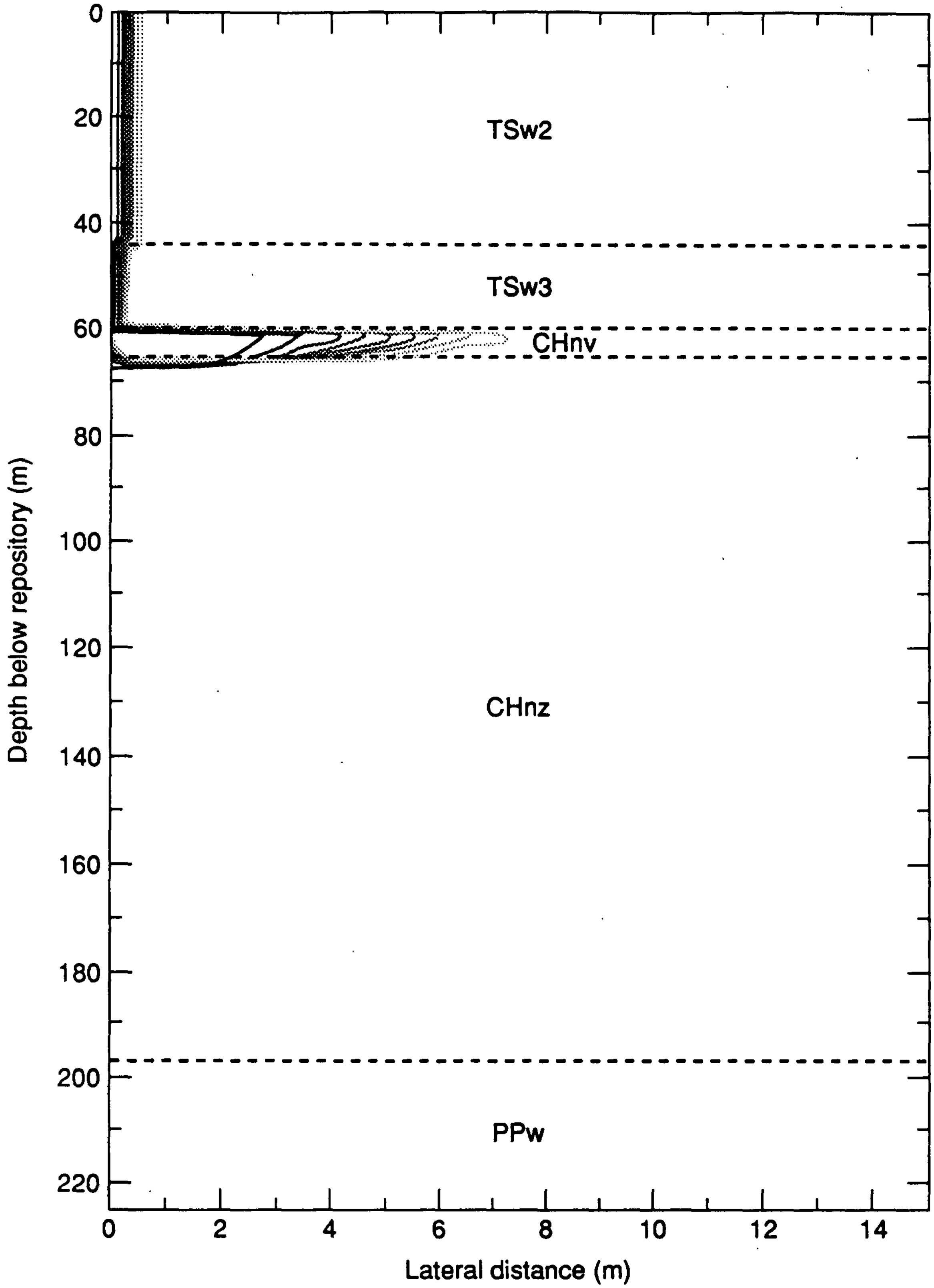

ES-TB-9 (2-18-91) IL

100 μm fracture; fracture spacing = 30 m
Dimensionless liquid saturation at t = 241 days

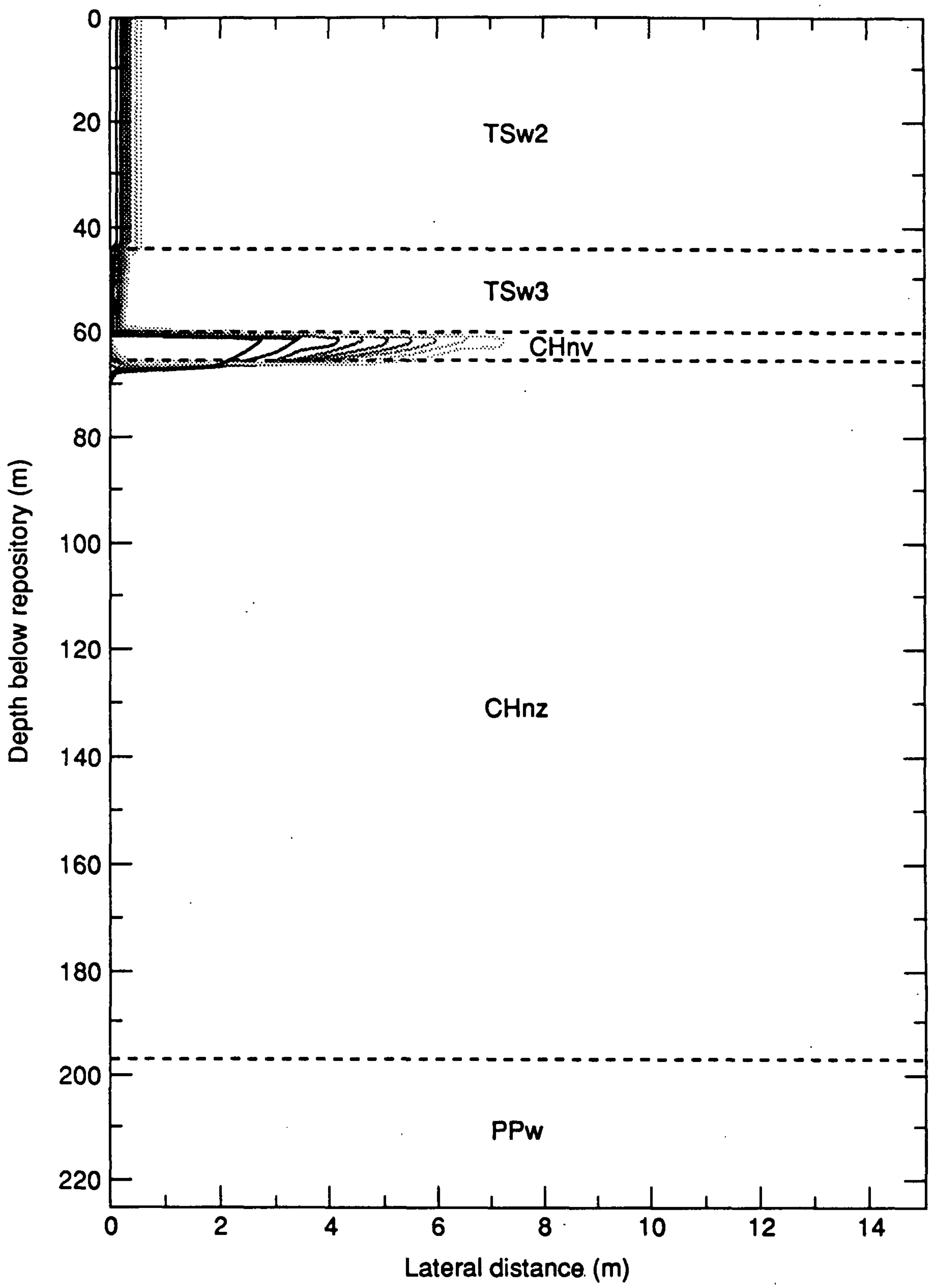

ES-TB-11 (2-20-91) IL

100 μm fracture; fracture spacing = 30 m
Dimensionless liquid saturation at t = 290 days

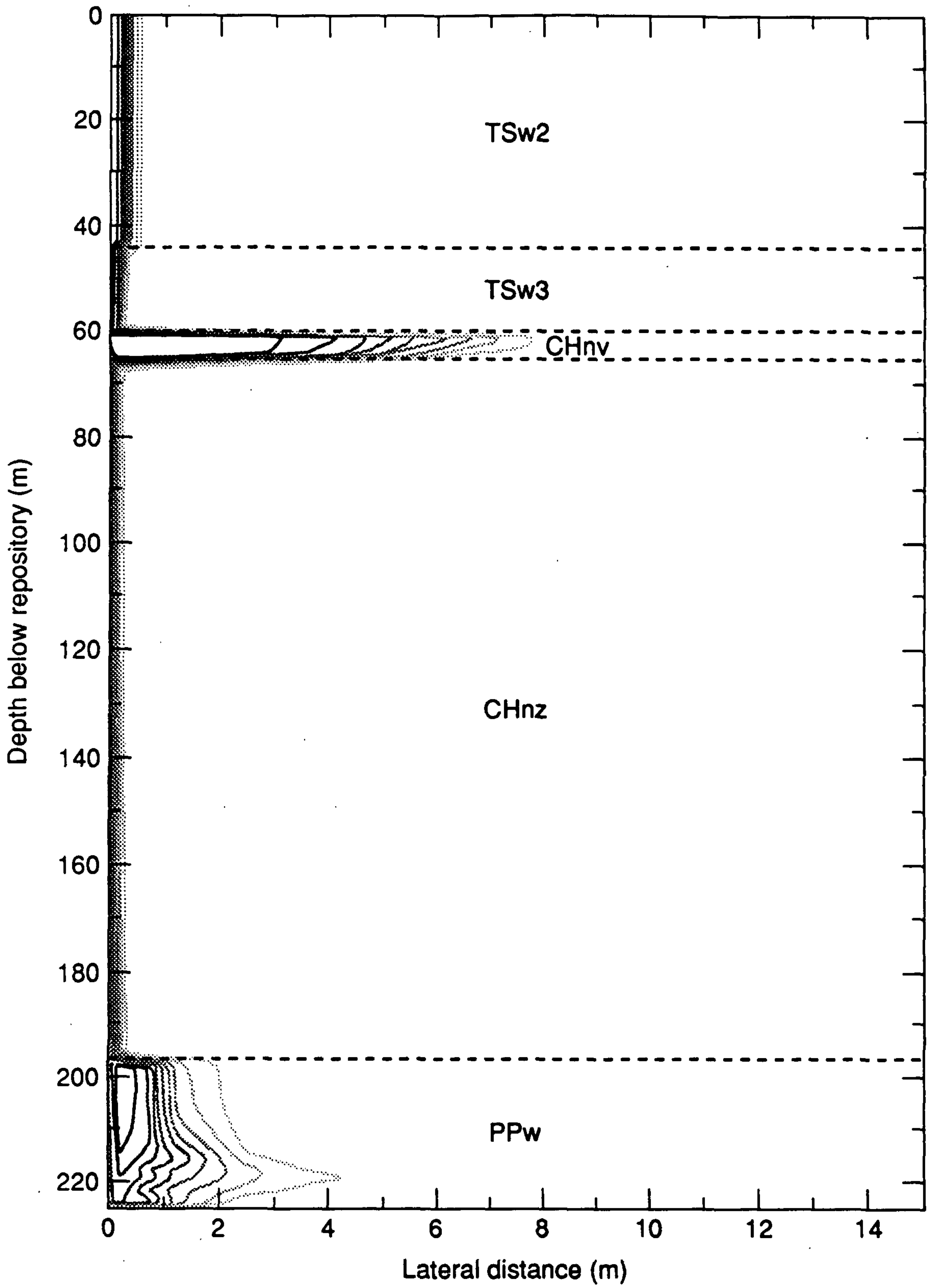

ES-TB-13 (2-18-91) IL

100 μm fracture; fracture spacing = 30 m; no CHnv
Dimensionless liquid saturation at t = 52 hours

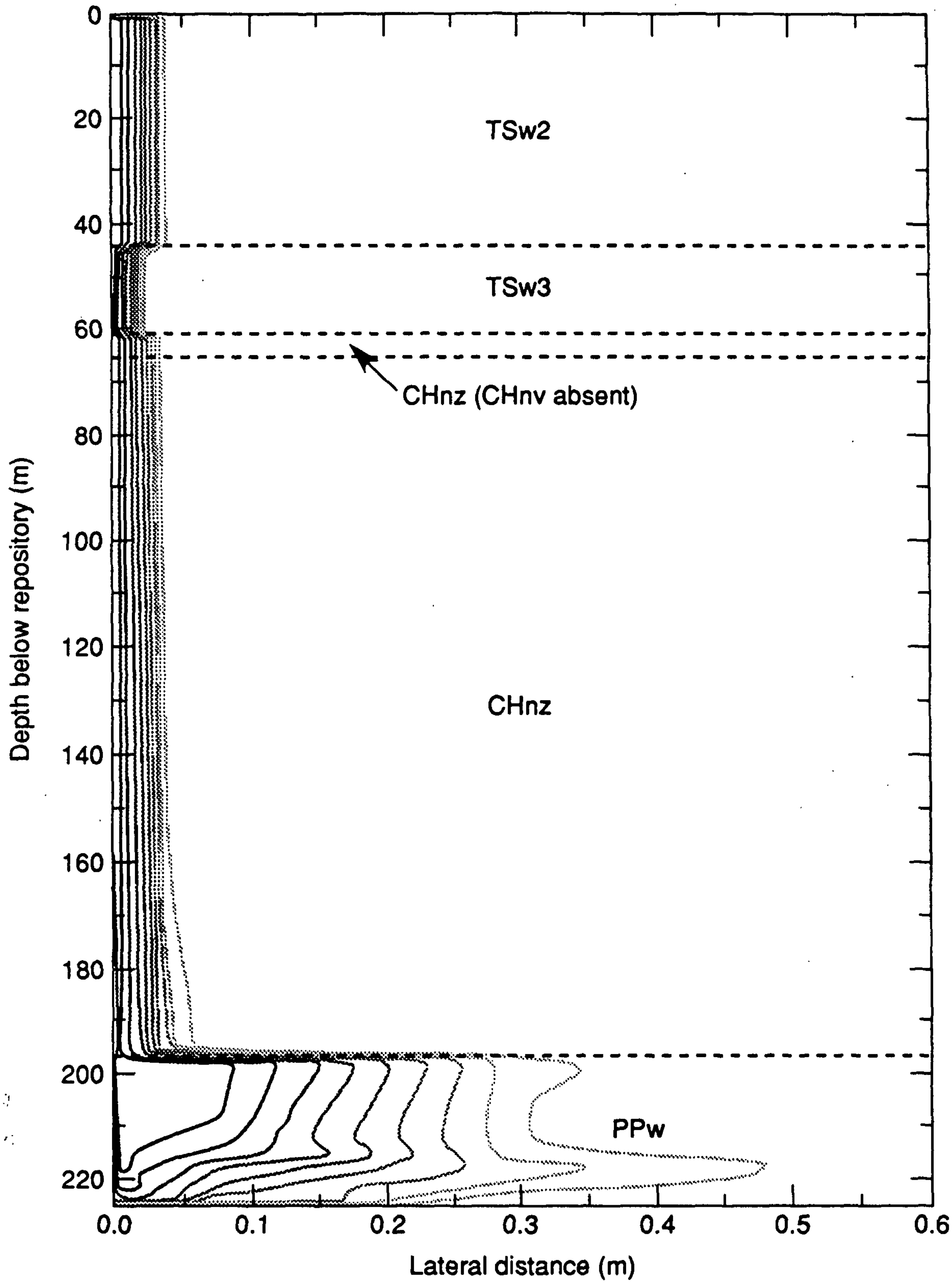

ES-TB-5 (3-1-91) IL

1000 μm fracture; fracture spacing = 0.3 m
Dimensionless liquid saturation at t = 350 s

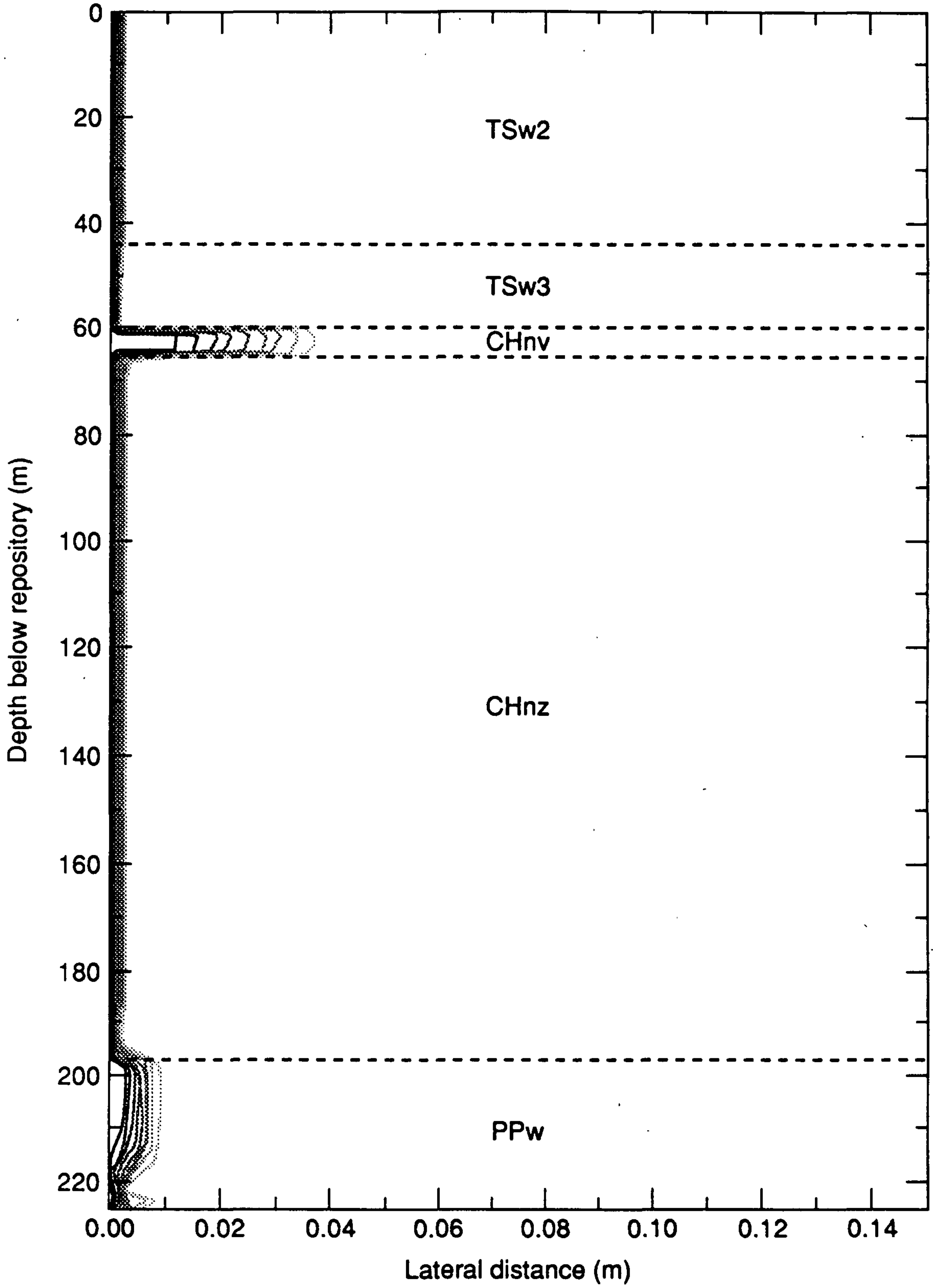

ES-TB-8 (2-18-91) IL

1000 μm fracture; fracture spacing = 0.3 m; no CHnv
Change in dimensionless liquid saturation at t = 260 s

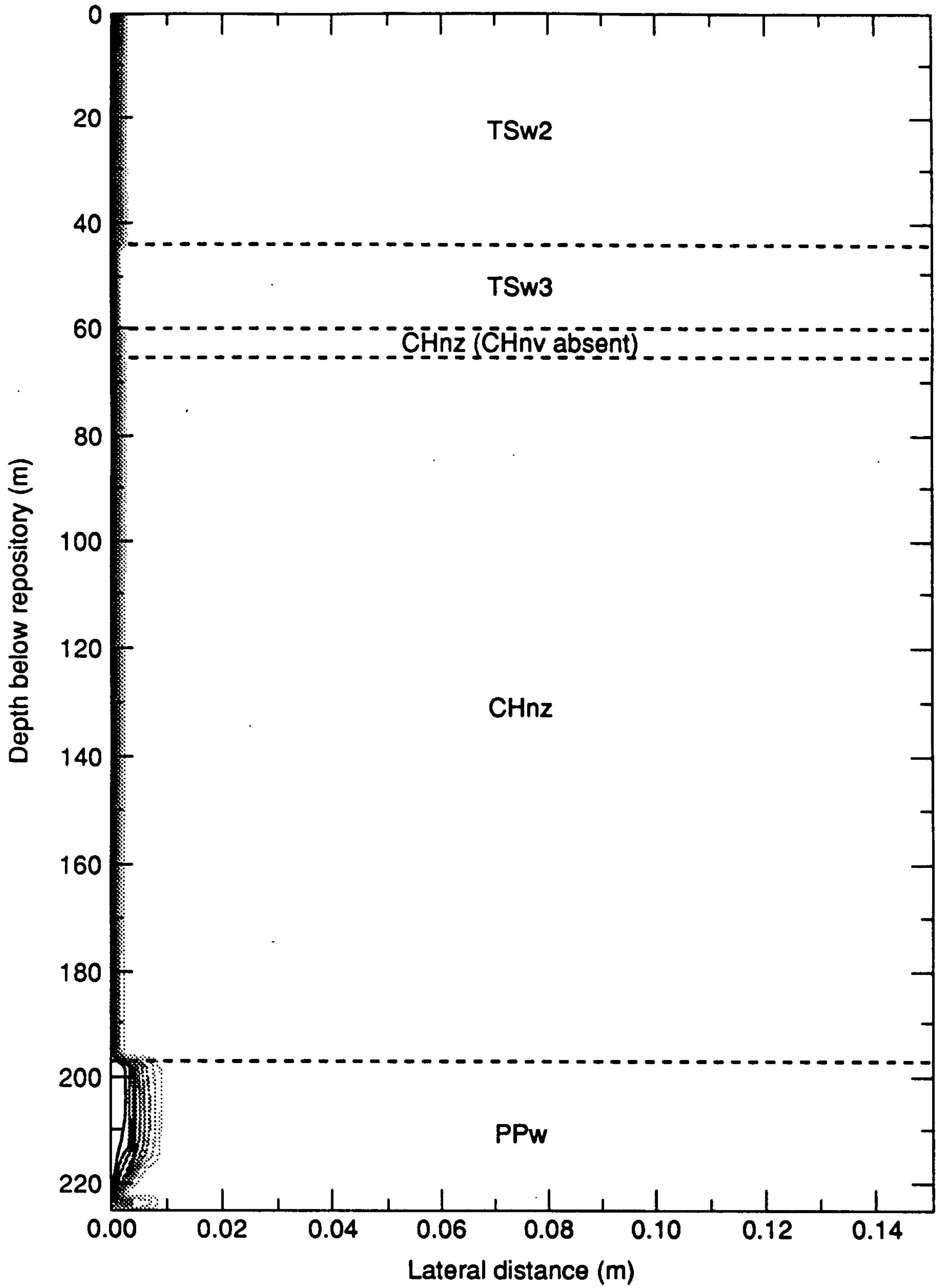

ES-TB-22 (3-20-91) IL

The maximum width of the wetting zone within a given hydrostratigraphic unit, d_m^* is extremely sensitive to the fracture aperture, b

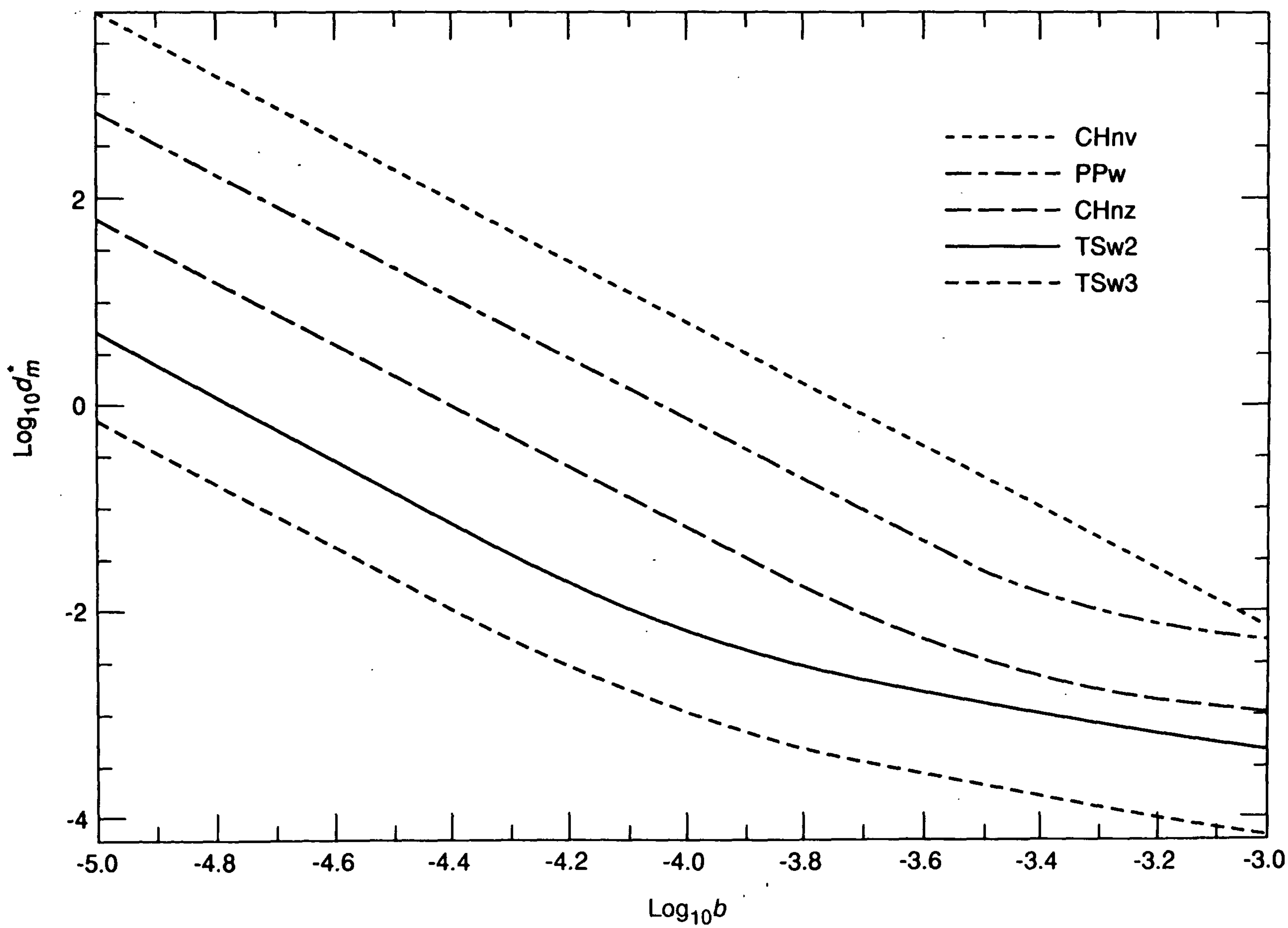

100 μm fracture; fracture spacing = 400. m
Dimensionless liquid saturation at t = 2.5 hours

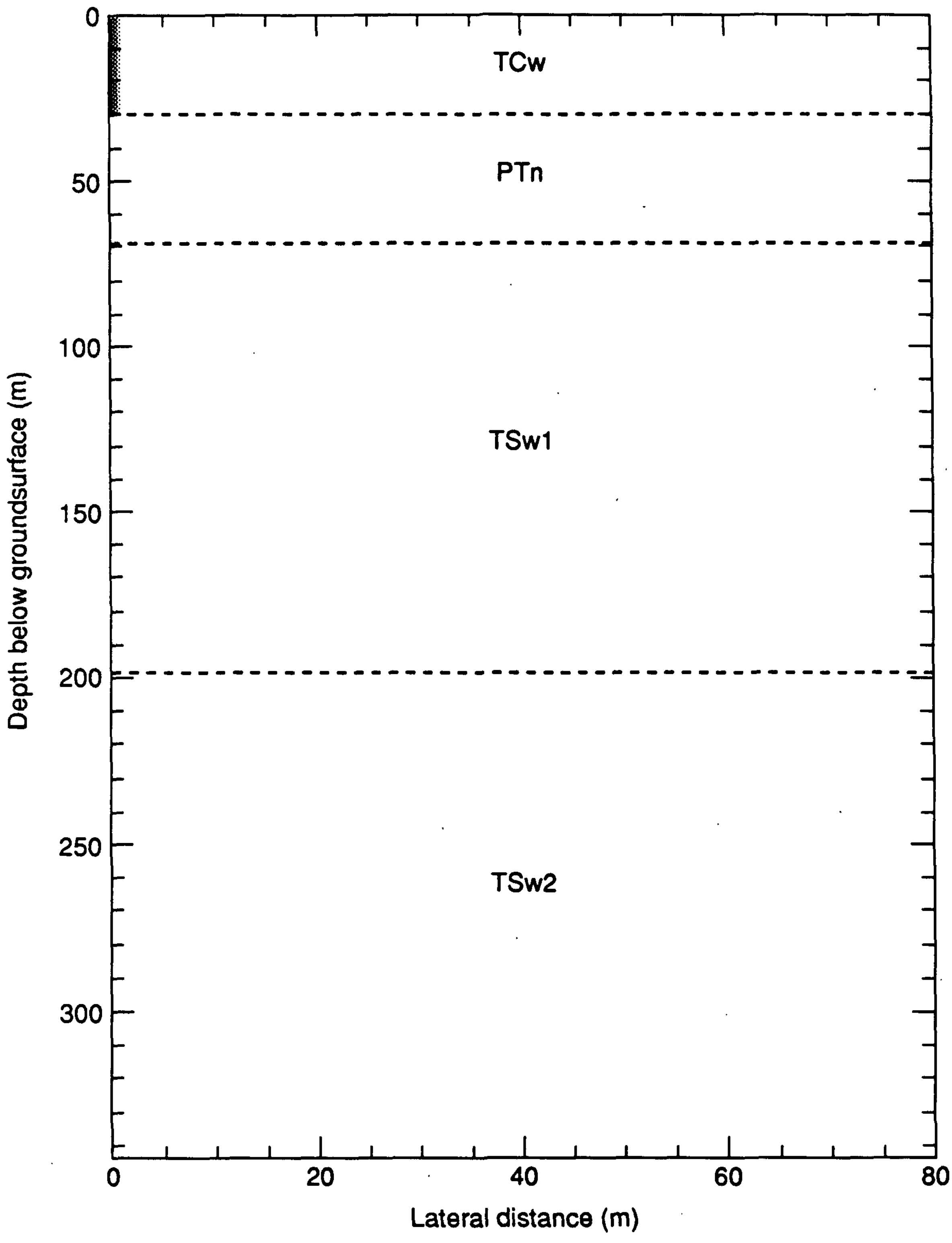

ES-TB-11 (3-12-91) IL

100 μm fracture; fracture spacing = 400. m
Dimensionless liquid saturation at t = 10 years

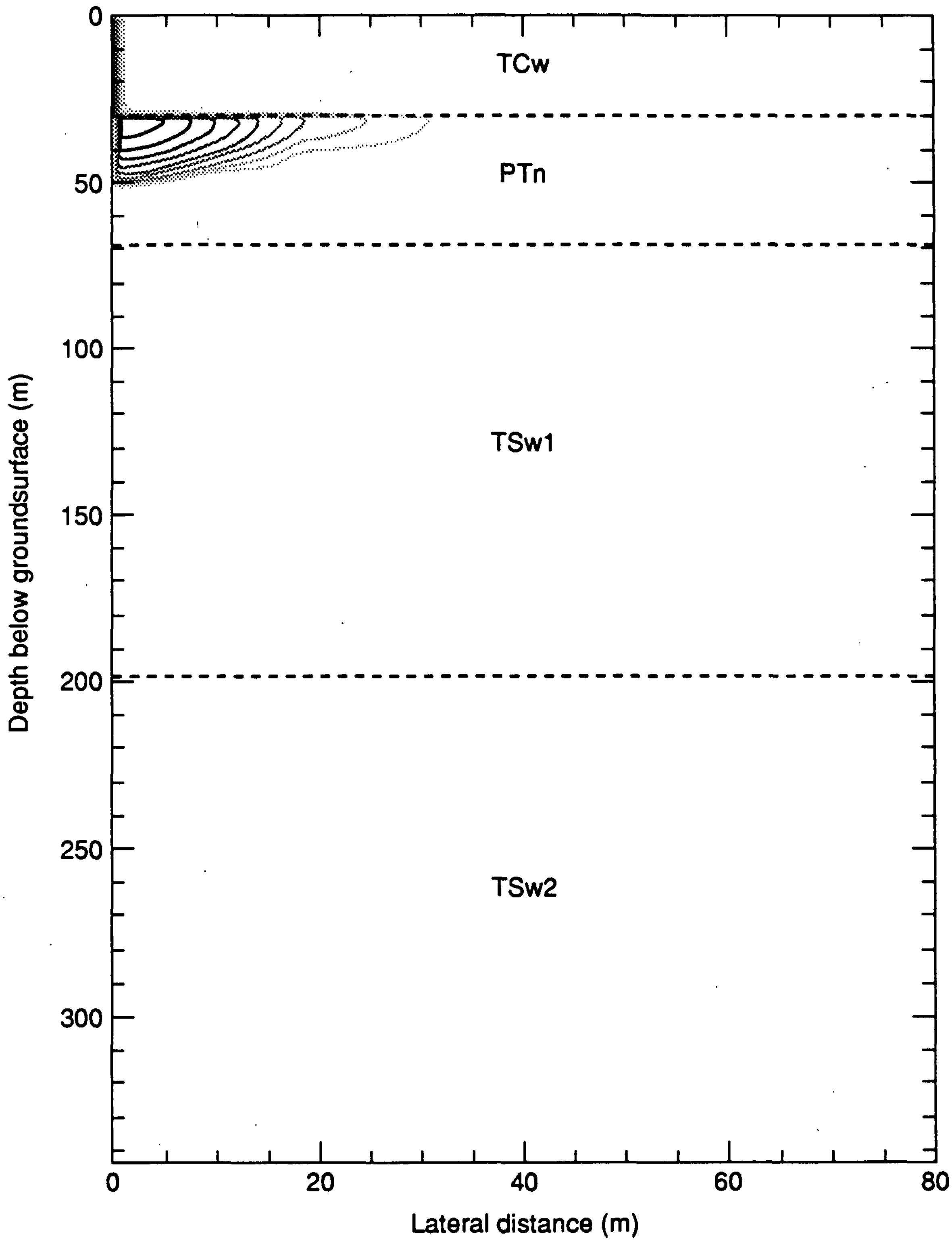

100 μm fracture; fracture spacing = 400. m
Dimensionless liquid saturation at t = 40 years

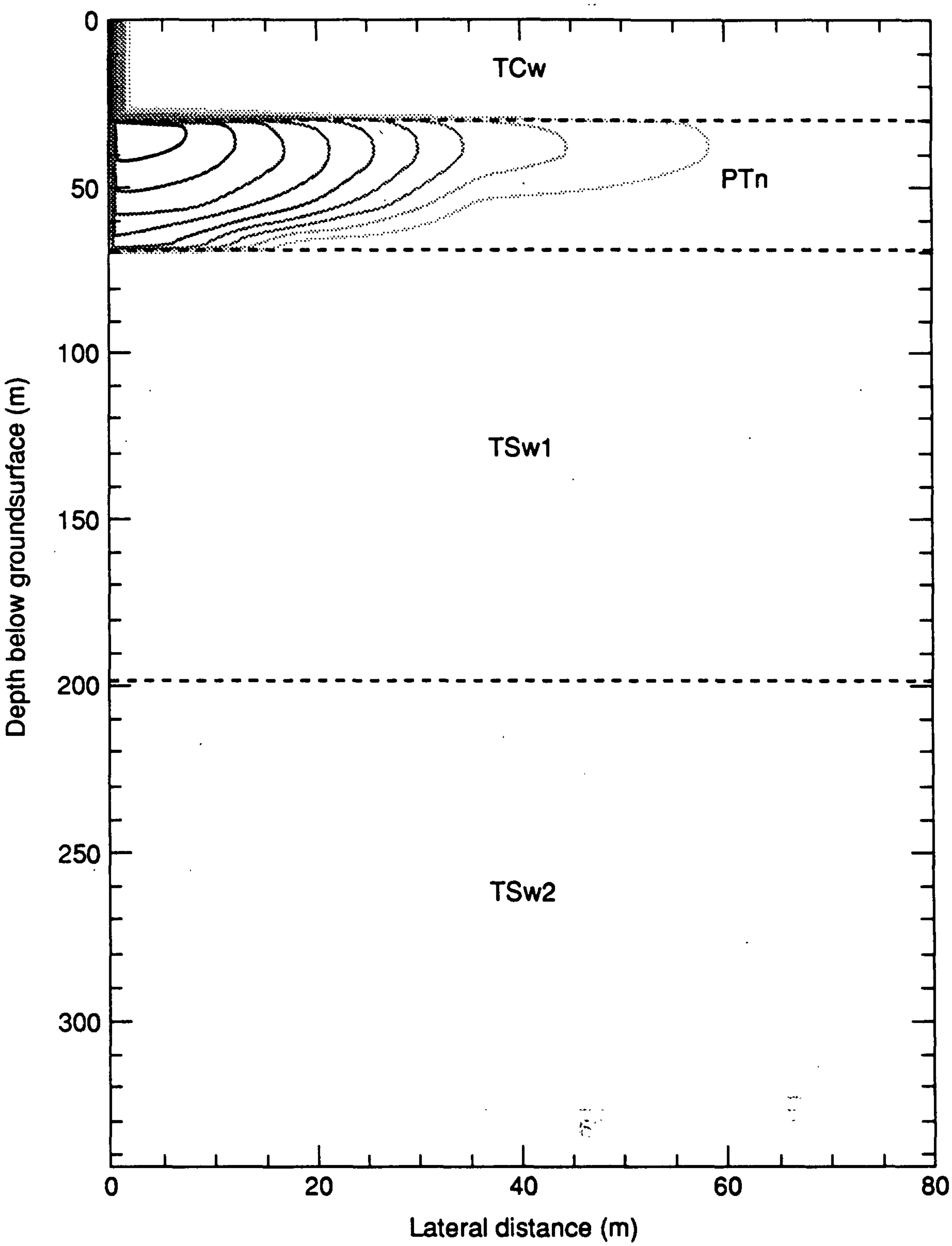

ES-TB-13 (3-12-91) IL

100 μm fracture; fracture spacing = 400. m
Dimensionless liquid saturation at t = 50 years

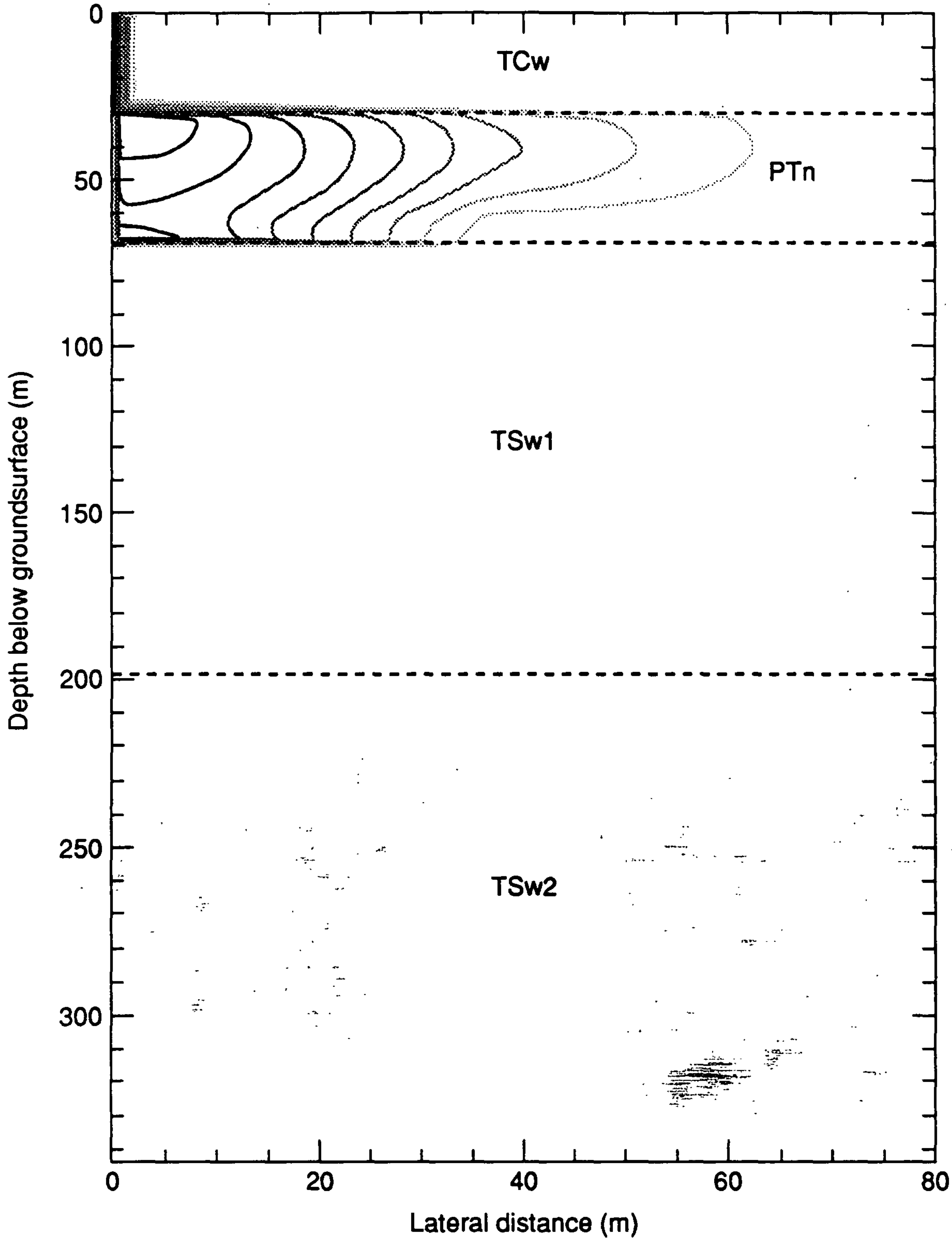

ES-TB-14 (3-13-91) IL

100 μm fracture; fracture spacing = 400. m
Dimensionless liquid saturation at t = 68 years

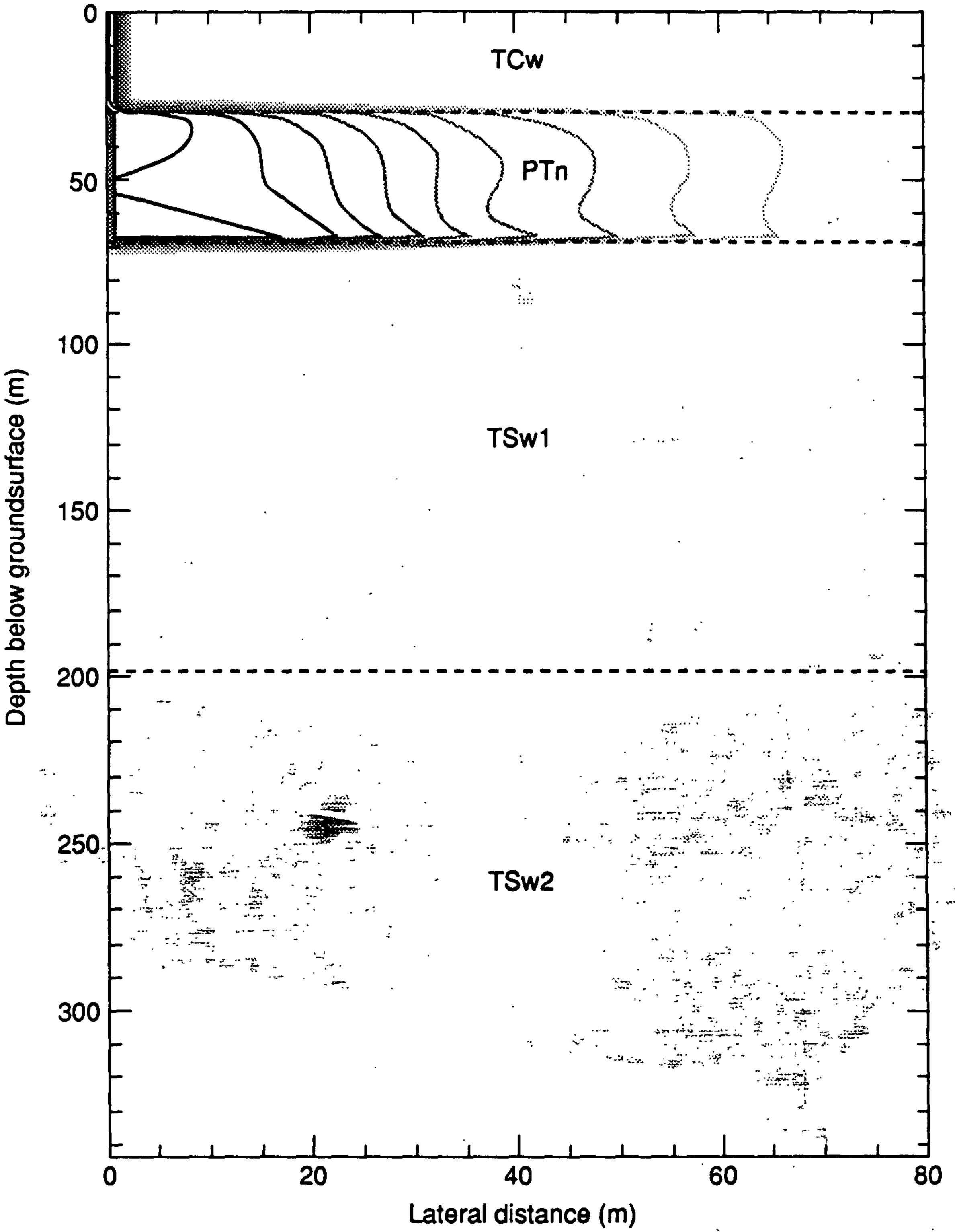

ES-TB-23 (3-26-91) IL

1000 μm fracture; fracture spacing = 3.0 m
Dimensionless liquid saturation at t = 30 sec

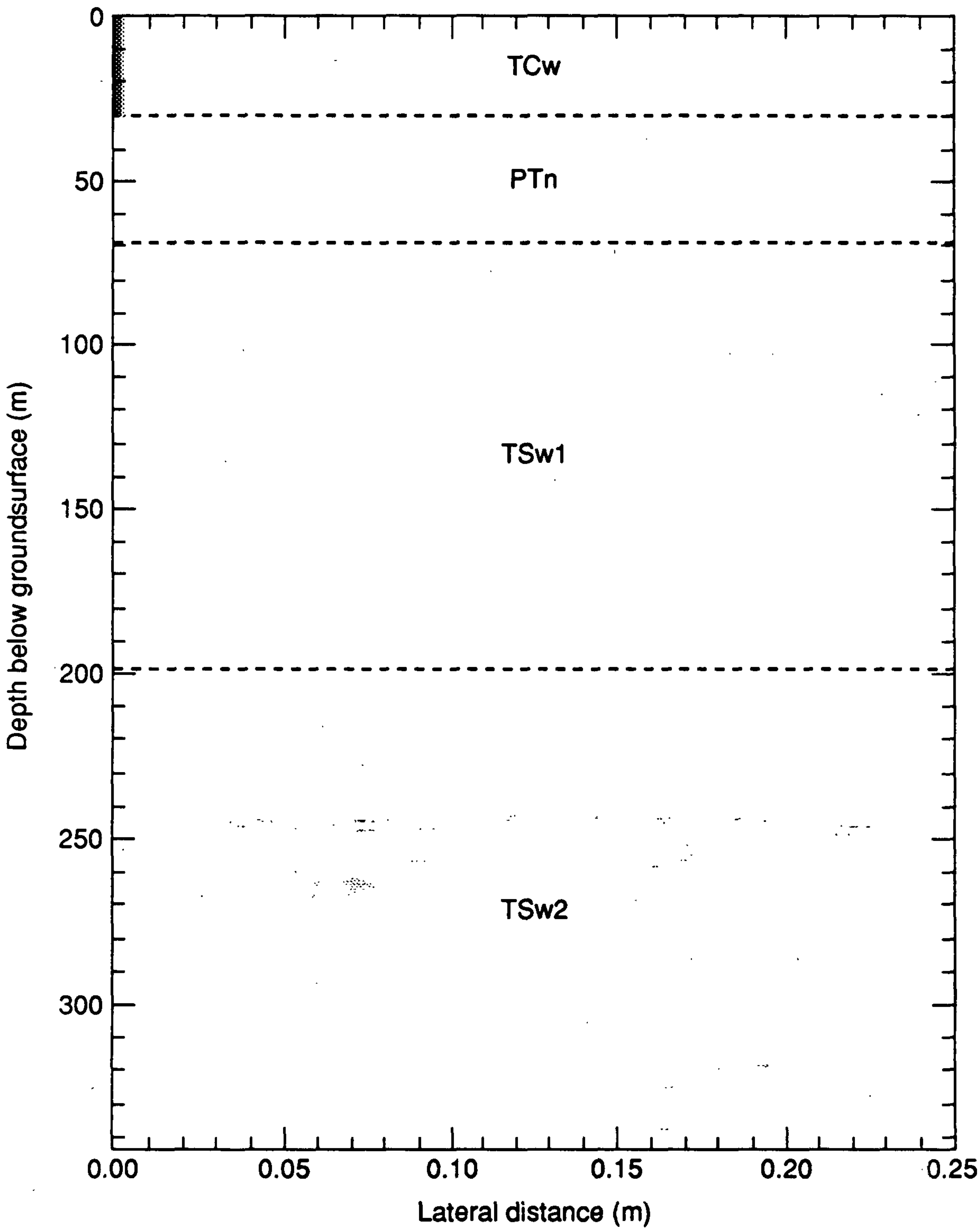

1000 μm fracture; fracture spacing = 3.0 m
Dimensionless liquid saturation at t = 2200 sec

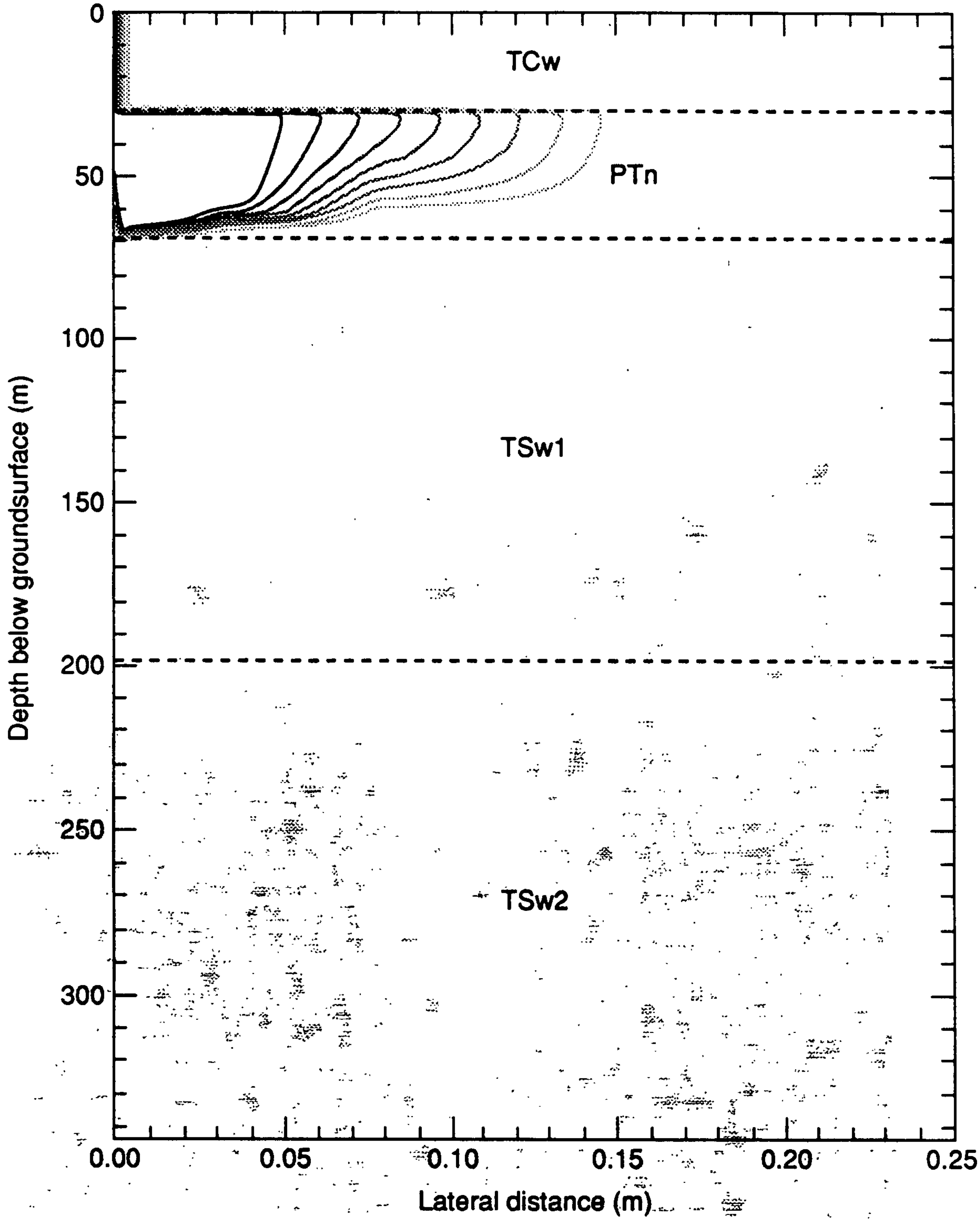

1000 μm fracture; fracture spacing = 3.0 m
Dimensionless liquid saturation at t = 1 hour

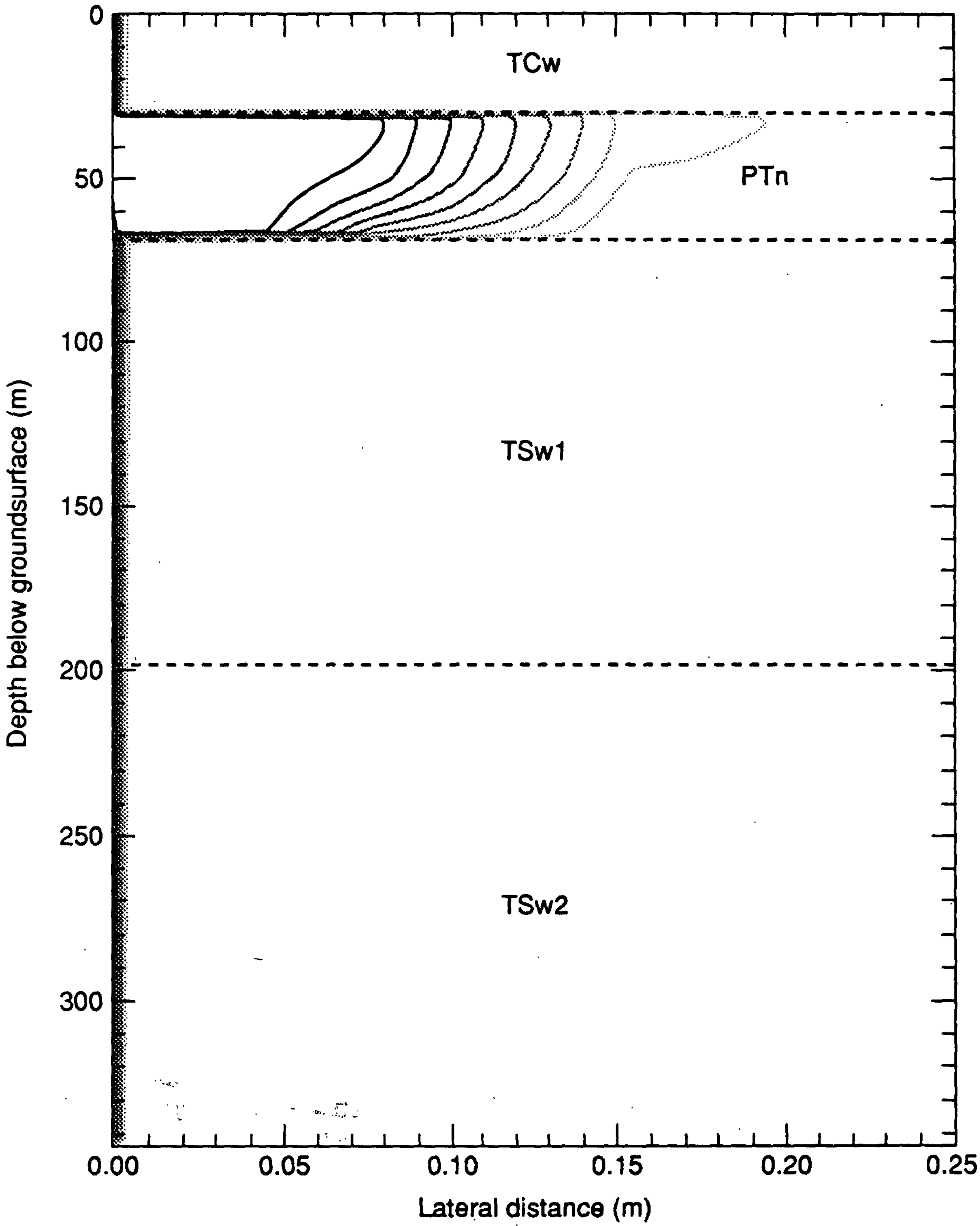

ES-TB-10 (3-12-91) IL

For a 100 µm fracture it takes from 100 to 10^4 times longer for a liquid pulse to reach the repository than it takes it to travel from the repository to the water table

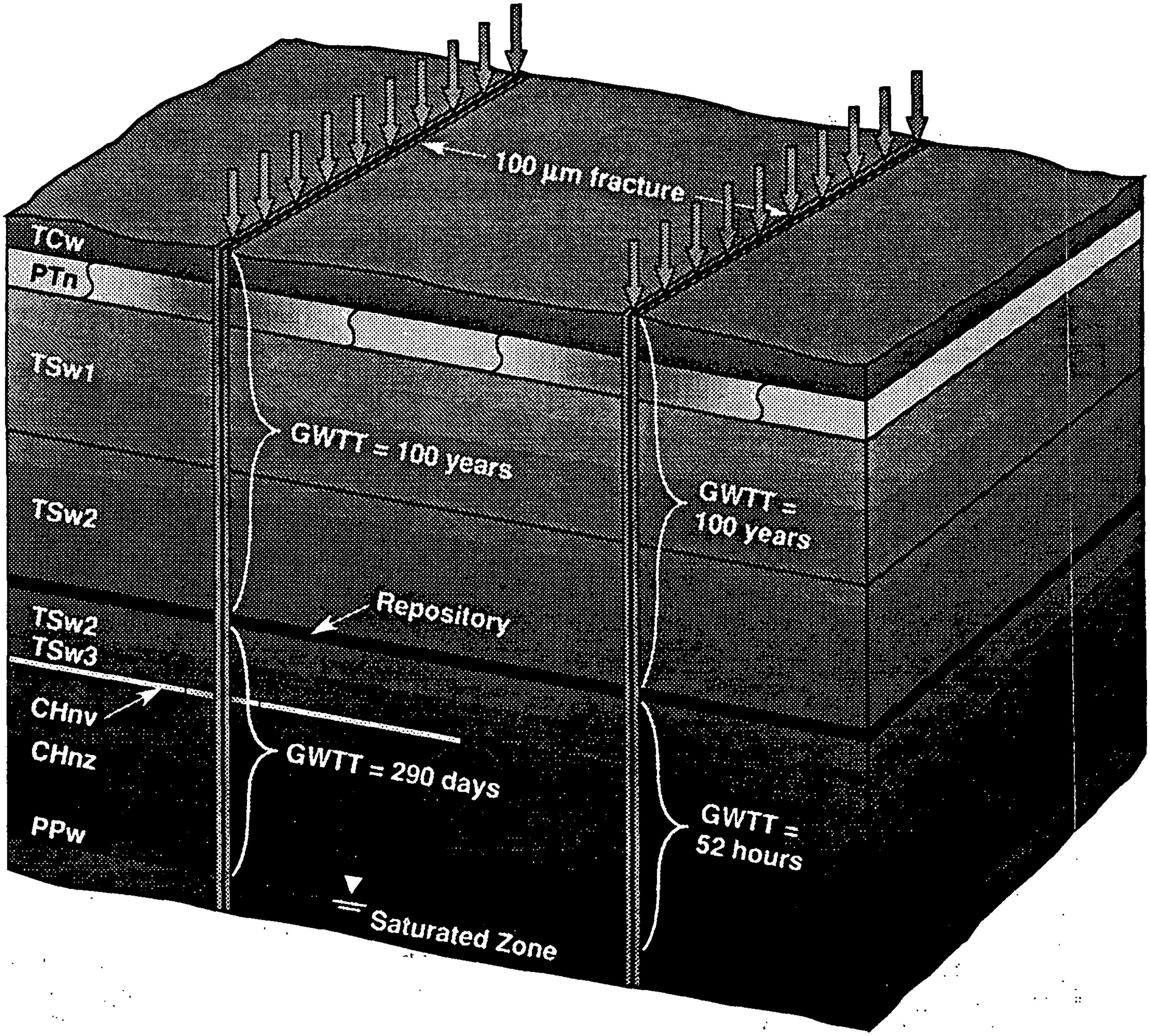

ES-TB-19 (3-7-91) FH

For a 1000 µm fracture it takes little more than one hour for a liquid pulse to reach the water table regardless of whether it penetrates the highly permeable CHnv unit

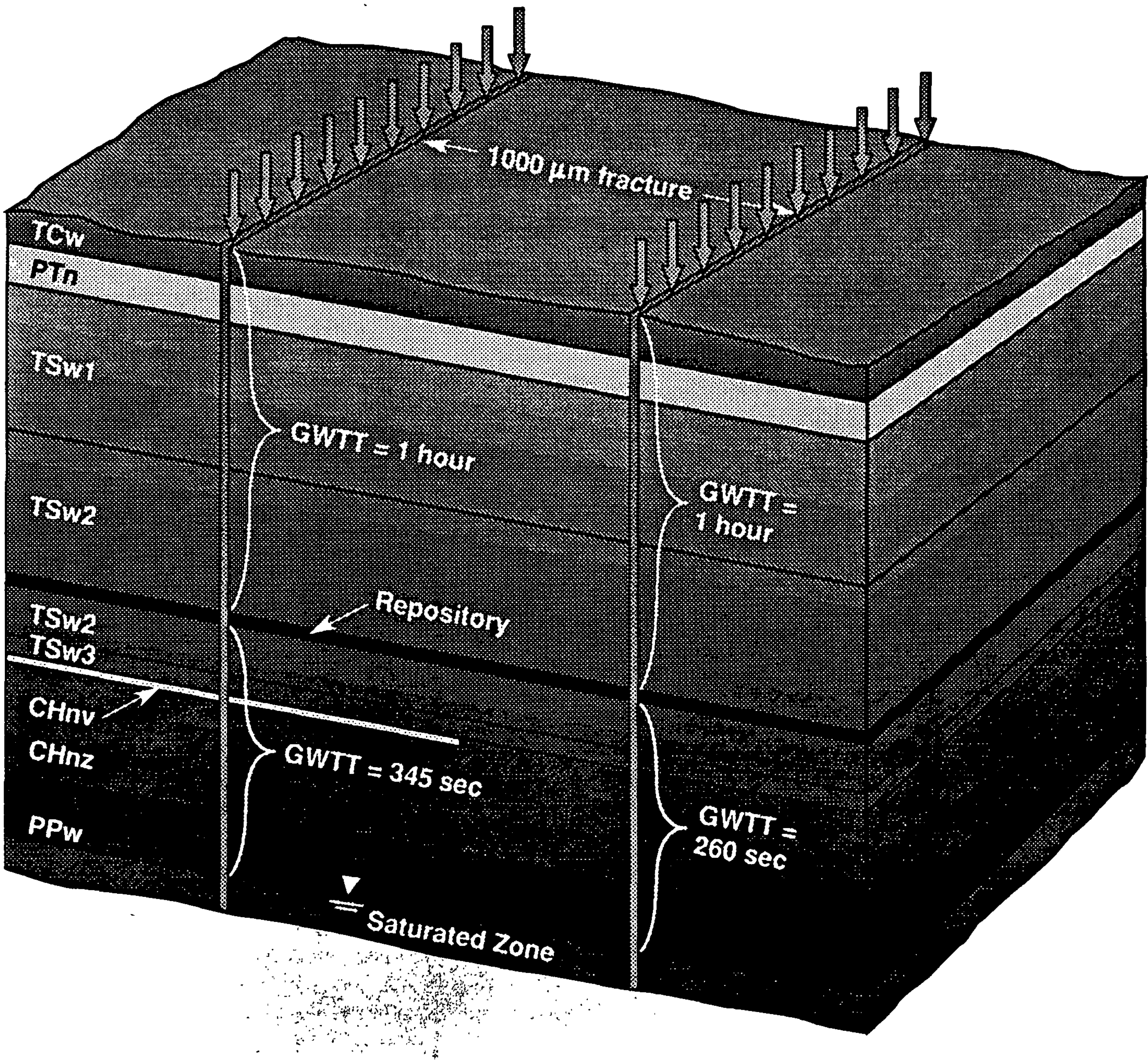

ES-TB-18 (3-7-91) FH

Episodic infiltration occurs as fracture-dominated flow in the low permeability units and matrix-dominated flow in the high permeability units (Buscheck and Nitao, 1991)

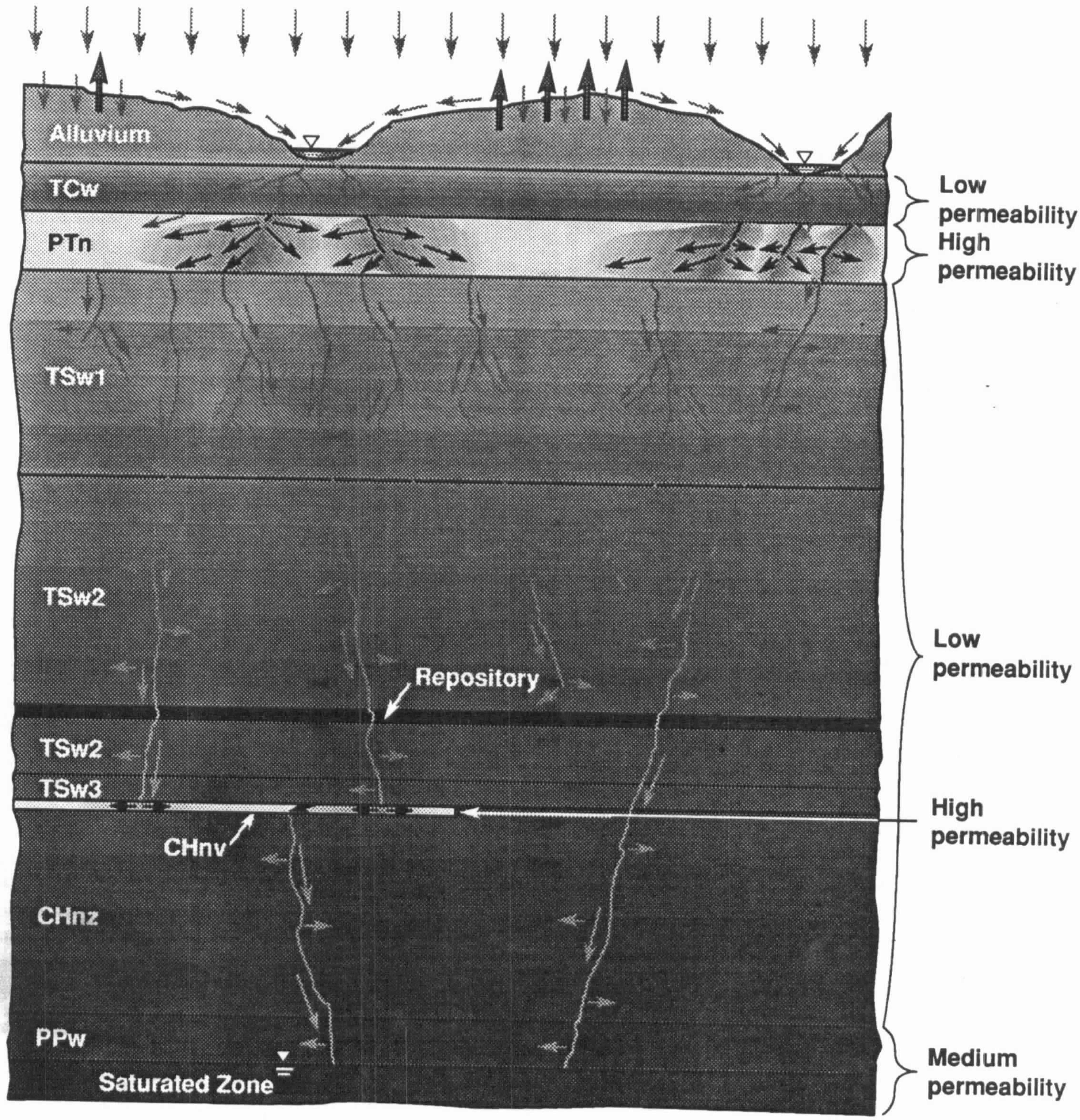

Greater fracture densities in the welded low permeability units may facilitate vapor phase removal of moisture (Buscheck and Nitao, 1991)

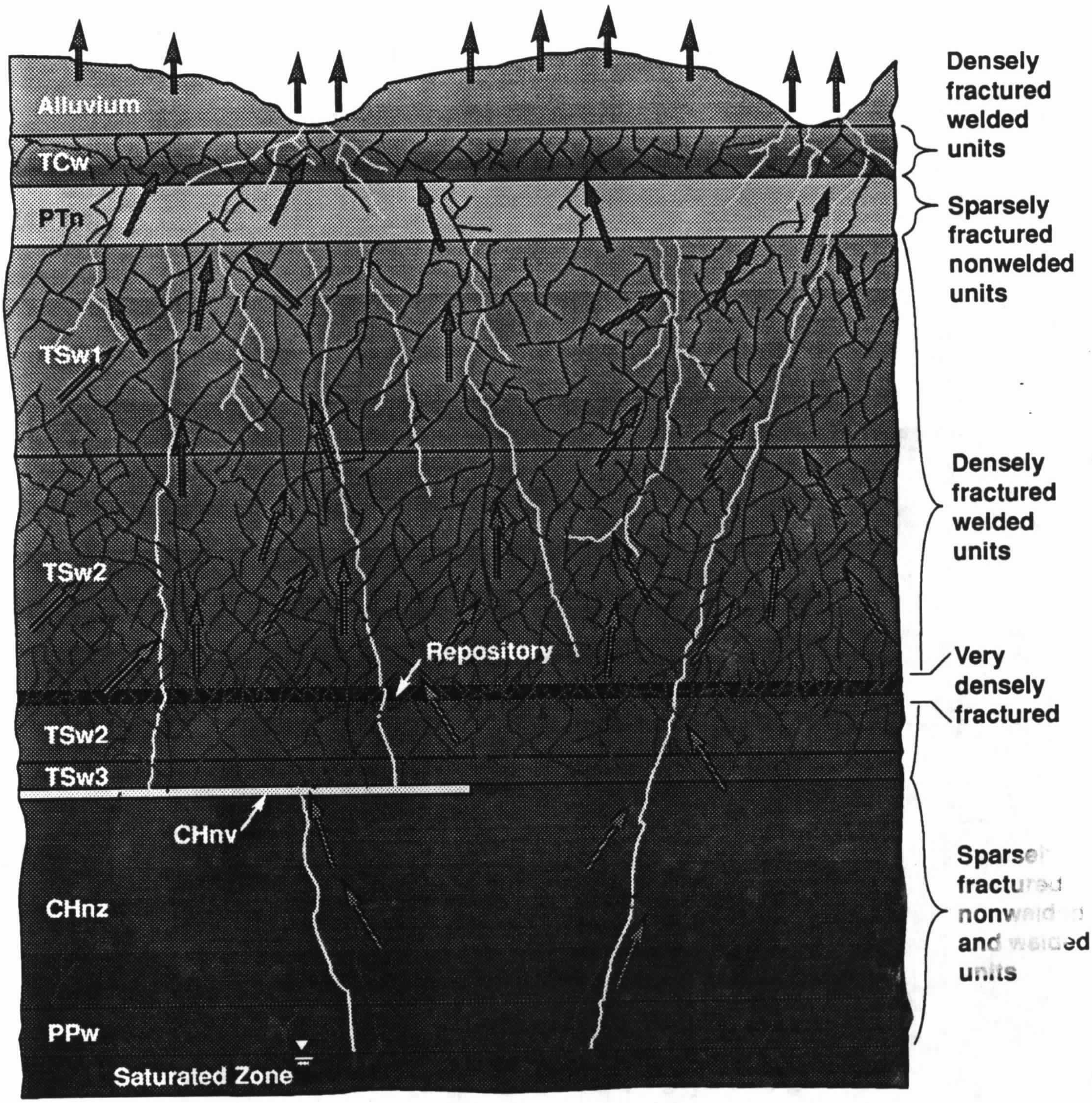

Fracture-Matrix Flow: Physical Retardation of Radionuclides

Impact of successive infiltration events

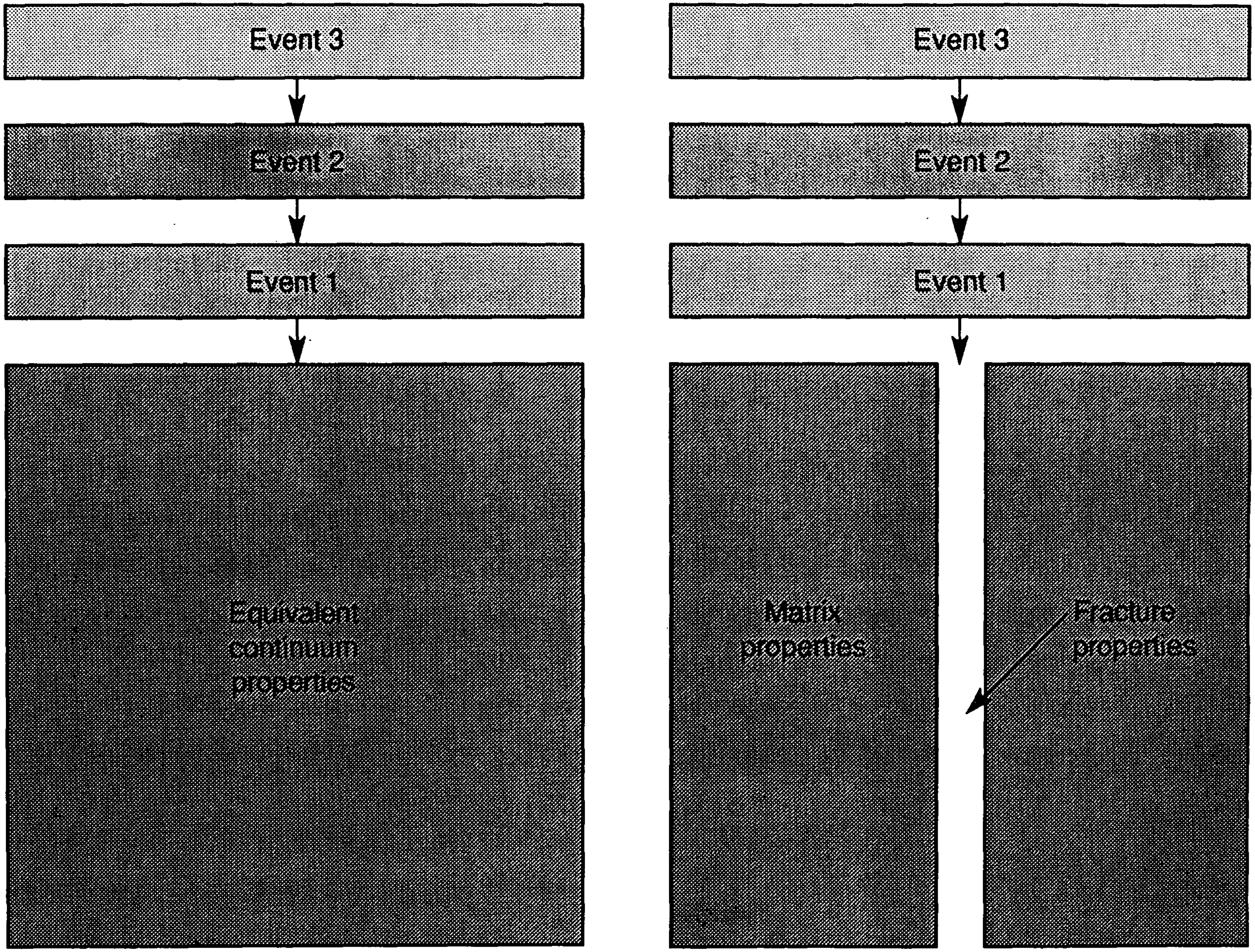

Equivalent continuum model smears radionuclide transport

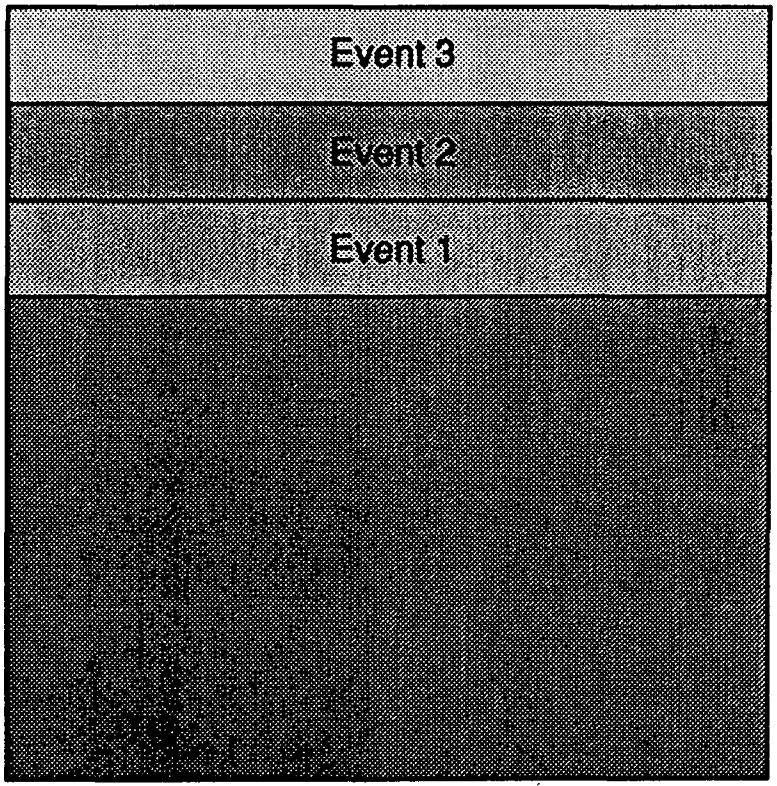

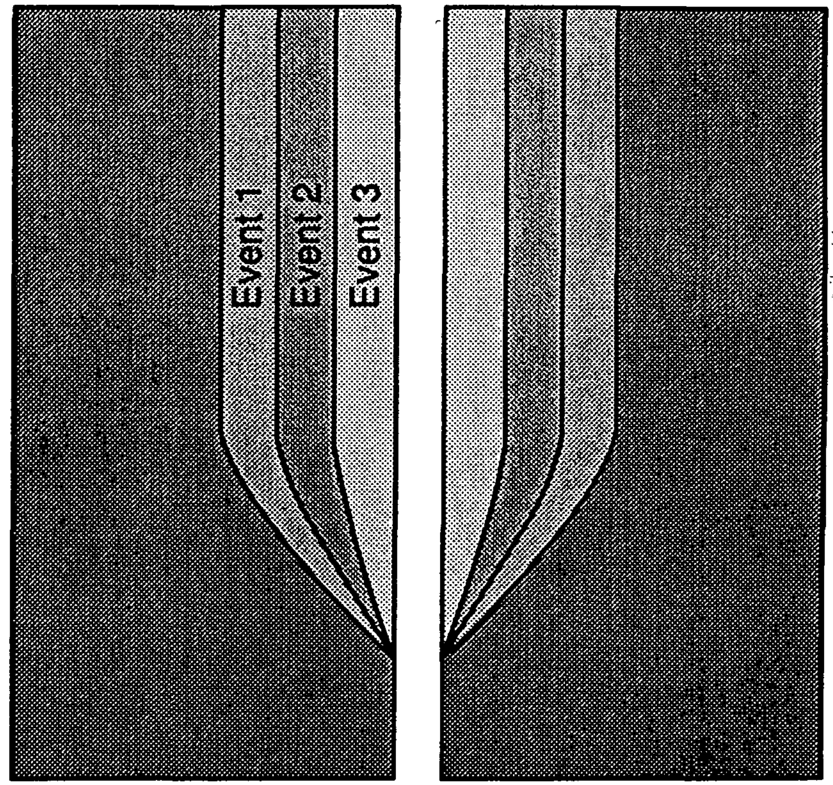

The Impact of Repository-Generated Hydrothermal Flow

The fracture system sheds condensate due to a combination of: (1) vapor flow away from the heat source and (2) gravity-driven liquid flow

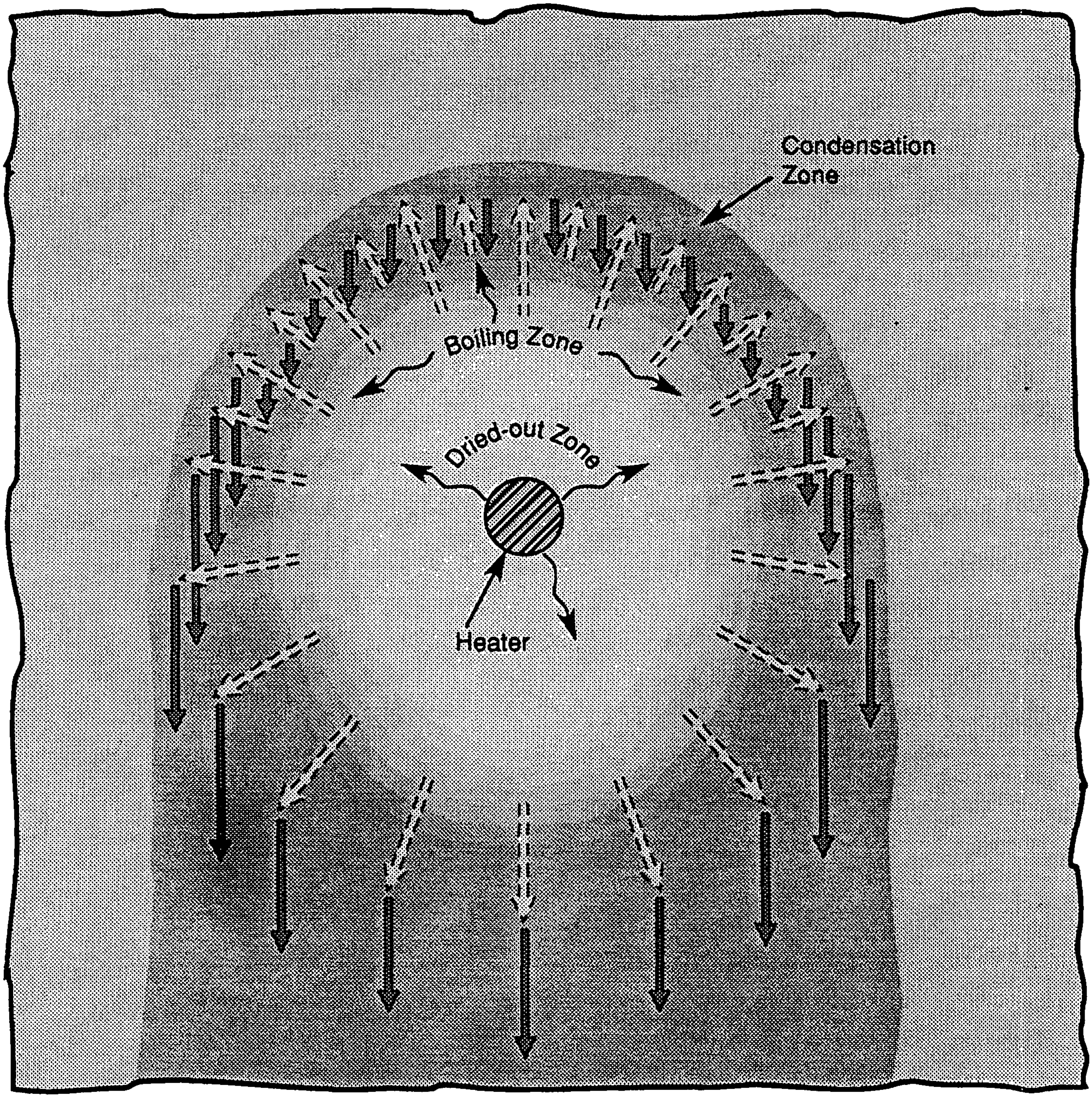

Under hydrothermally perturbed conditions, boiling will mitigate episodic fracture flow from reaching the waste package (for up to 1000 years for a repository heat loading rate of 57 *kw/acre*) (Buscheck and Nitao, 1991)

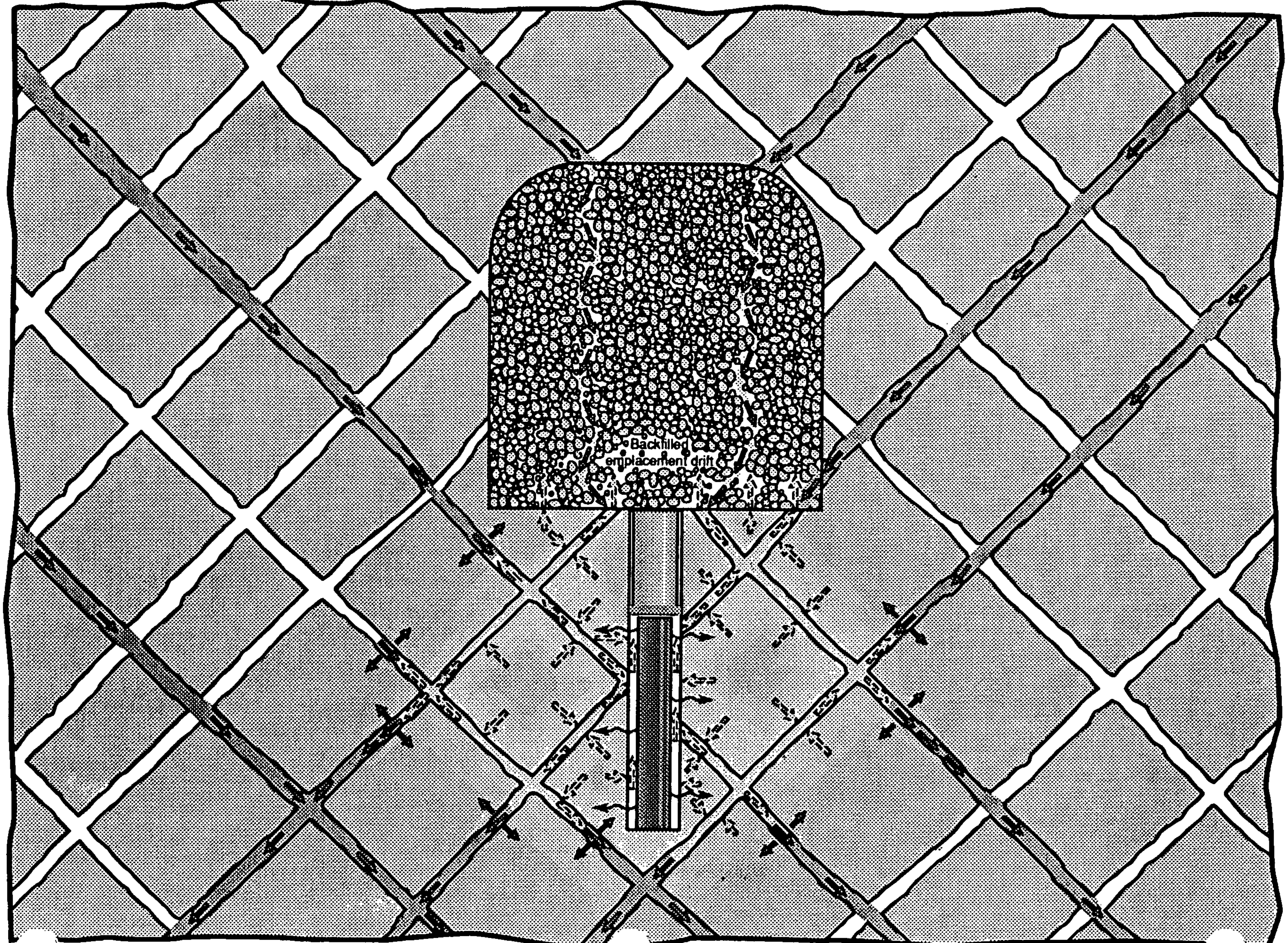

ES-TB-7 (4-20-91) IL

Net condensate generation flux averaged over entire repository for 15-ft center-to-center spacing of 10, 20, 40, 60, and 80-year-old PWR spent fuel

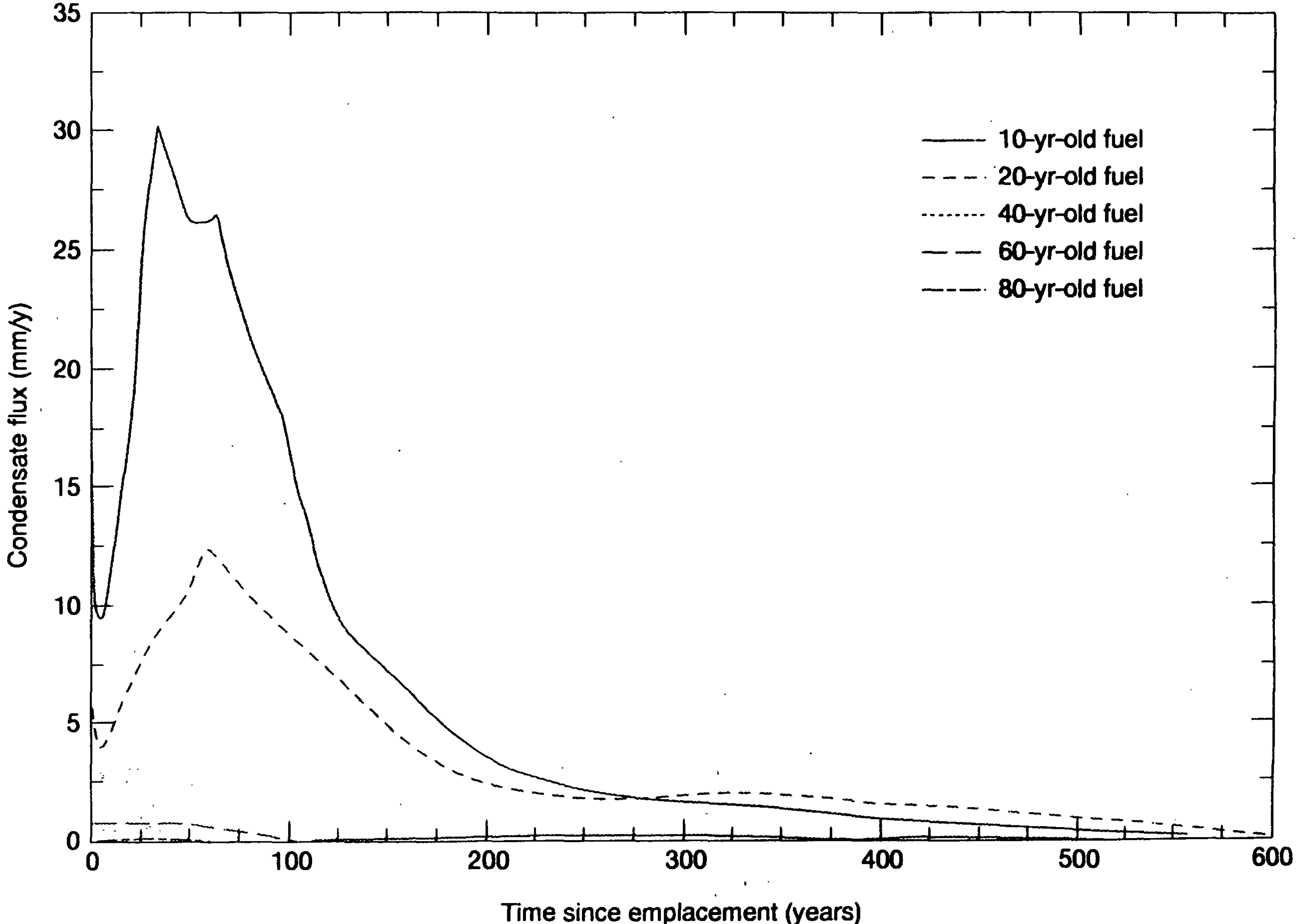

ES-TB-38 (6-15-91) IL

Under nominal conditions, neglecting hydrothermal perturbations allows episodic fracture flow to reach the waste package (Buscheck and Nitao, 1991)

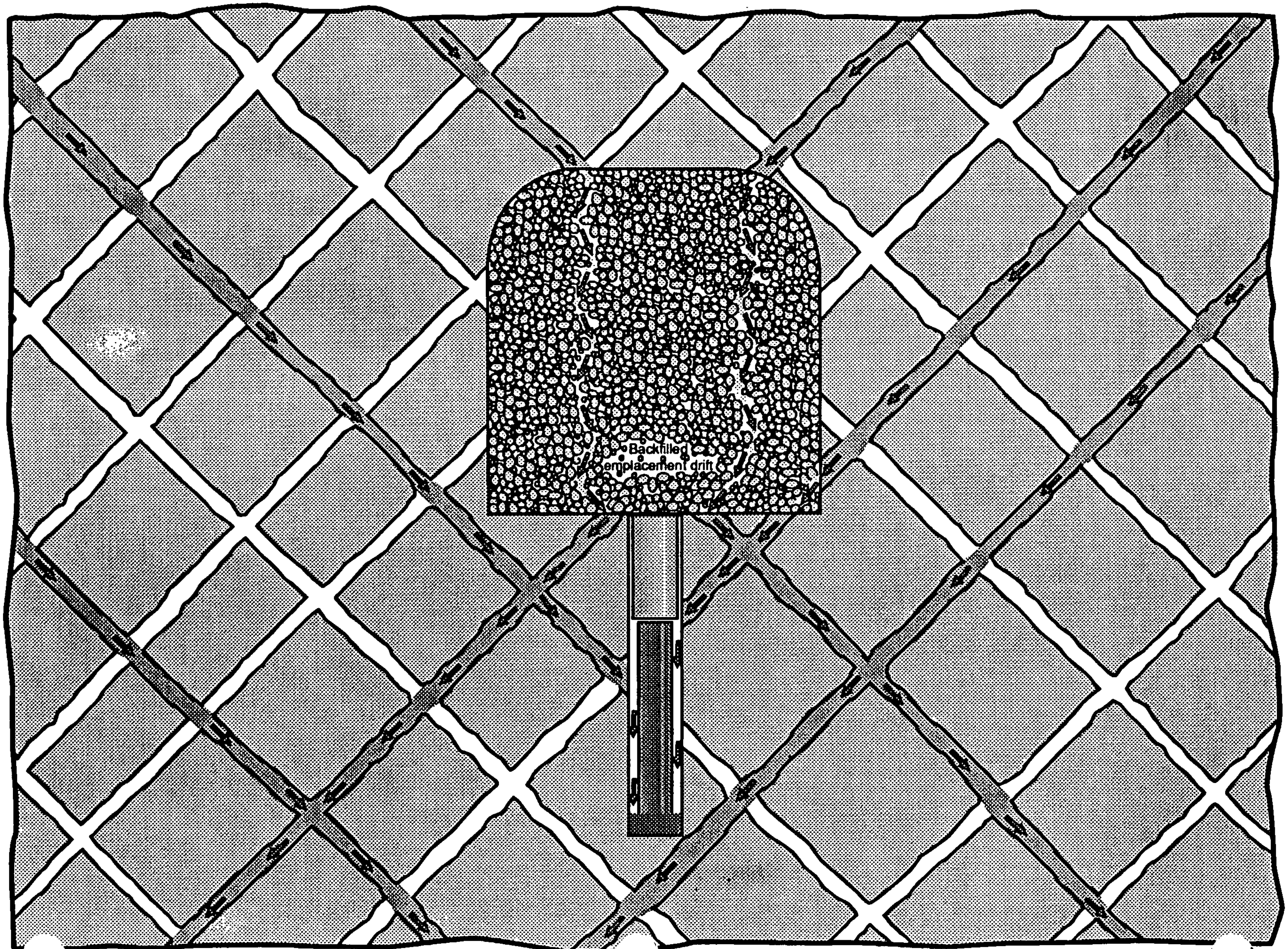

ES-TB-9 (4-20-91) IL

Engineered backfill with high moisture sorbing material (e.g. crushed nonwelded PTn tuff) will mitigate episodic fracture flow from reaching the waste package (Buscheck and Nitao, 1991)

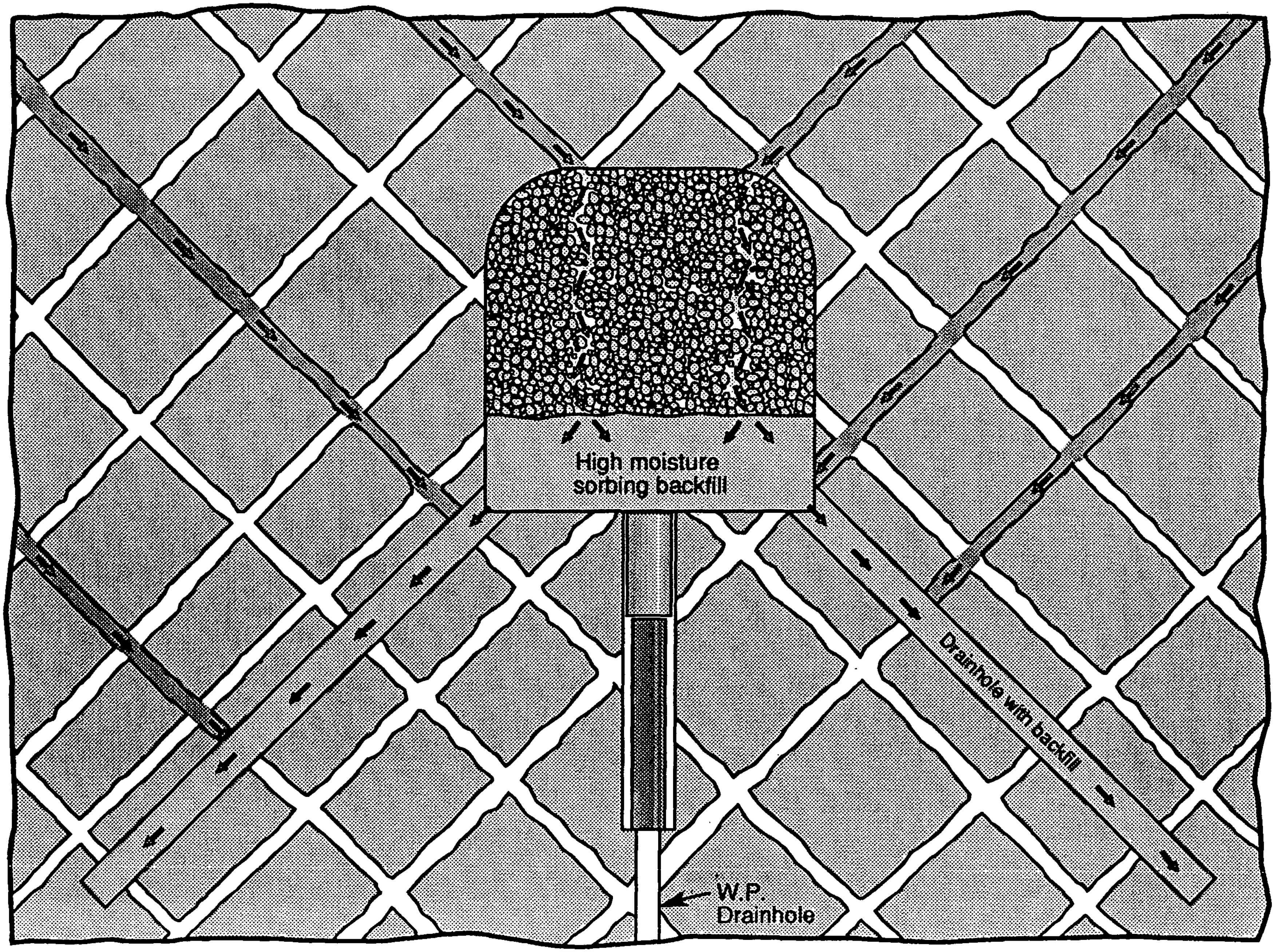

ES-TB-10 (4-20-91) IL

Conclusions

The importance of fracture-dominated flow

- Due to the small matrix permeability, matrix-dominated flow will not result in significant vertical movement of radionuclides

- Field evidence indicates nonequilibrium fracture-matrix flow can occur to considerable depths

Conclusions

Fracture-dominated versus matrix-dominated flow

- Matrix-dominated flow occurs when the flux is sufficiently low such that flow in the matrix keeps up with flow in the fracture

- Fracture-dominated flow occurs when the flux is sufficiently high such that the liquid front in the fracture moves in advance of the flow in the matrix

Conclusions

Fracture-dominated flow: episodic behavior

- Due to matrix imbibition, little additional liquid front movement occurs in the fracture following removal on an infiltration source

- For episodic events separated by a few days, the cumulative liquid front movement in the low matrix permeability units is nearly the same had all events occurred consecutively

- For the high matrix permeability units episodic events can be separated by several years without affecting the cumulative liquid front movement

- A key consideration affecting radionuclide movement is the intensity and duration of the maximum possible infiltration episode

Conclusions

Summary of fracture-matrix flow in Yucca Mountain

- Due to the small matrix permeability, fracture-dominated flow is likely in the welded TCw, TSw1, TSw2, TSw3 units and the zeolitized nonwelded CHnz unit

- Due to the large matrix permeability, matrix-dominated flow is likely in the vitric nonwelded PTn and CHnv units

- The high matrix permeability of the vitric nonwelded tuffs results in substantial lateral flow

- Contiguous fracture networks may facilitate significant vapor-phase removal of moisture from Yucca Mountain

Conclusions

Summary of fracture-matrix flow in Yucca Mountain (continued)

- 99 to 99.99 percent of Yucca Mountain's capacity to retard fracture flow by virtue of matrix imbibition exists above the repository horizon

- Prioritization and planning of site characterization activities should emphasize units dominating fracture flow retardation (i.e. the PTn)

Conclusions

Physical retardation of radionuclides

- Shortly following an episodic infiltration event, liquid in the fracture will be totally imbibed by the matrix
- Matrix imbibition mitigates vertical displacement of radionuclides (imbibed during earlier events) by subsequent events
- If a radionuclide front is not driven to the water table during the course of an infiltration episode, then its subsequent vertical movement will be governed by matrix-dominated flow

Conclusions

Repository-generated hydrothermal flow

- The boiling zone acts as a "hydrothermal" umbrella, shielding the waste packages from condensate drainage

- Depending on the heat loading at the repository, condensate drainage may constitute the dominant source of liquid flux at and below the repository horizon for hundreds of years

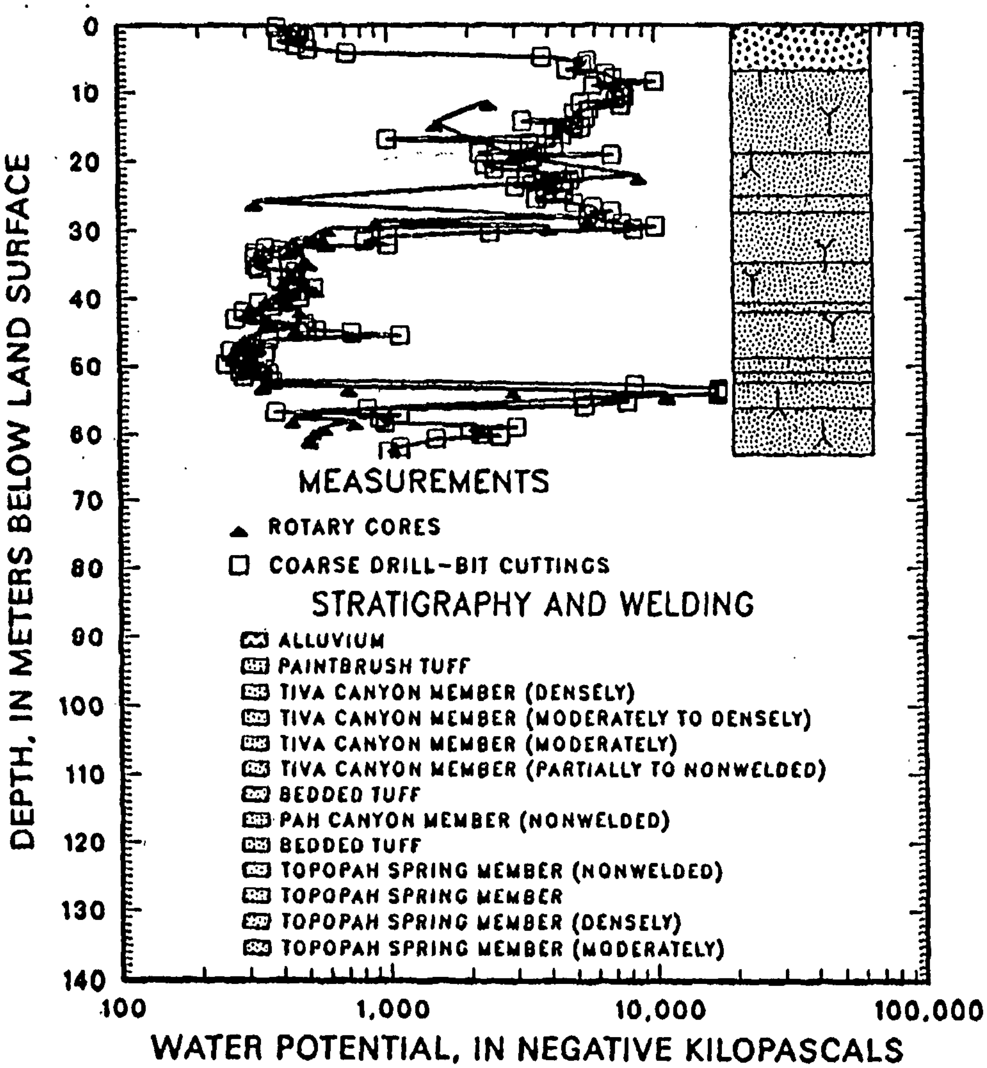

Figure 6.--Water-potential measurements, stratigraphy, and welding of rotary cores and coarse drill-bit cuttings from test hole USW UZ-7.

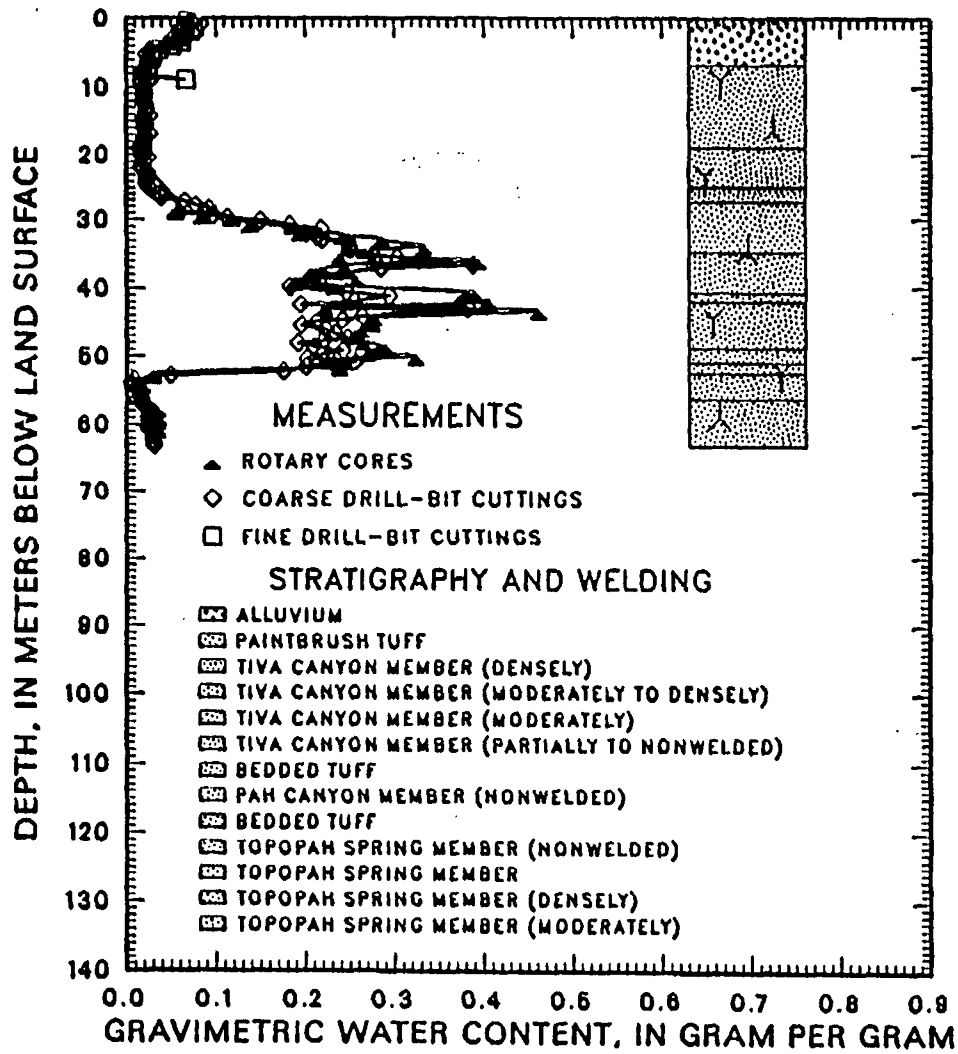

Figure 4.--Gravimetric water-content measurements, stratigraphy, and welding of rotary cores and drill-bit cuttings from test hole USW UZ-7.